

Stable and Scalable Spectral Element Methods

Paul Fischer

*Mathematics and Computer Science Division
Argonne National Laboratory*

Joint work with:

Fausto Cattaneo

James Lottes

Misun Min

Chaman Verma

Frank Loth UIC

Aleks Obabko U Chicago

and numerous others...

Overview

- ❑ High-order motivation: minimal dispersion/dissipation
- ❑ Efficiency – matrix-free factored forms
 - solvers: MG-preconditioned CG or GMRES
- ❑ Stability – high-order filters
 - dealiasing (i.e., “proper” integration)
- ❑ Scalability – long time integration
 - bounded iteration counts
 - scalable coarse-grid solvers (sparse-basis projection or AMG)
 - design for $P > 10^6$ ($P > 10^5$ *already here...*)
- ❑ Examples – vascular flows
 - MHD
 - Rod bundle flows

Navier-Stokes Time Advancement

$$\begin{aligned}\frac{\partial \mathbf{u}}{\partial t} + \mathbf{u} \cdot \nabla \mathbf{u} &= -\nabla p + \nu \nabla^2 \mathbf{u} \\ \nabla \cdot \mathbf{u} &= 0\end{aligned}$$

- ❑ Nonlinear term: *explicit*
 - ❑ k th-order backward difference formula / extrapolation
 - ❑ characteristics (*Pironneau '82, MPR '90*)

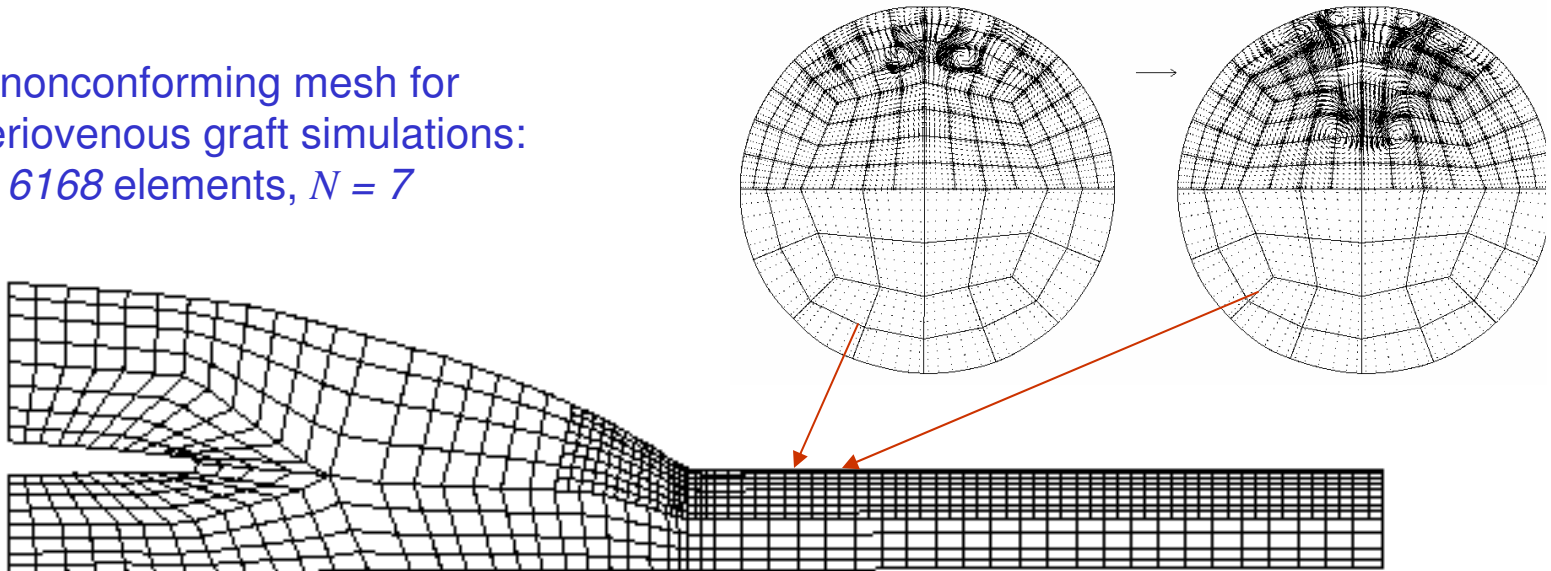
- ❑ Stokes problem – pressure/viscous decoupling, $P_N - P_{N-2}$ (*Maday & Patera 89*)
 - ❑ 3 Helmholtz solves for velocity – Jacobi-preconditioned CG
 - ❑ (consistent) Poisson equation for pressure (*computationally dominant*)

Spatial Discretization: *Spectral Element Method*

(Patera 84, Maday & Patera 89)

- ❑ Variational method, similar to FEM, using *GL* quadrature.
- ❑ Domain partitioned into E high-order quadrilateral (or hexahedral) elements (decomposition may be nonconforming - *localized refinement*)
- ❑ Trial and test functions represented as N th-order tensor-product polynomials within each element. ($N \sim 4$ -- 15, typ.)
- ❑ EN^3 gridpoints in 3D, EN^2 gridpoints in 2D.
- ❑ Converges *exponentially fast* with N for smooth solutions.

3D nonconforming mesh for
arteriovenous graft simulations:
 $E = 6168$ elements, $N = 7$



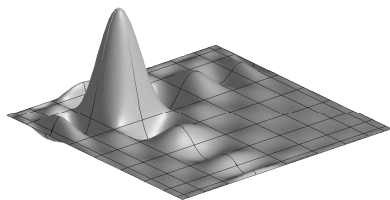
Spectral Element Discretization

$$u_t + \mathbf{c} \cdot \nabla u = \nu \nabla^2 u$$

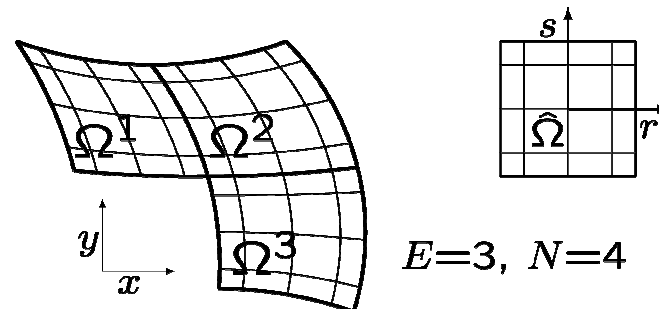
Find $u \in X_0^N \subset H_0^1$ such that

$$(v, u_t)_N + (v, \mathbf{c} \cdot \nabla u)_M = \nu (\nabla v, \nabla u)_N \quad \forall v \in X_0^N,$$

- $(f, g)_M := \sum_{j=0}^M \rho_j^M f(\xi_j^M) g(\xi_j^M)$, (1-D, $\Omega = [-1, 1]$)
- ξ_j^M, ρ_j^M — M th-order Gauss-Legendre points, weights.



2D basis function, $N=10$



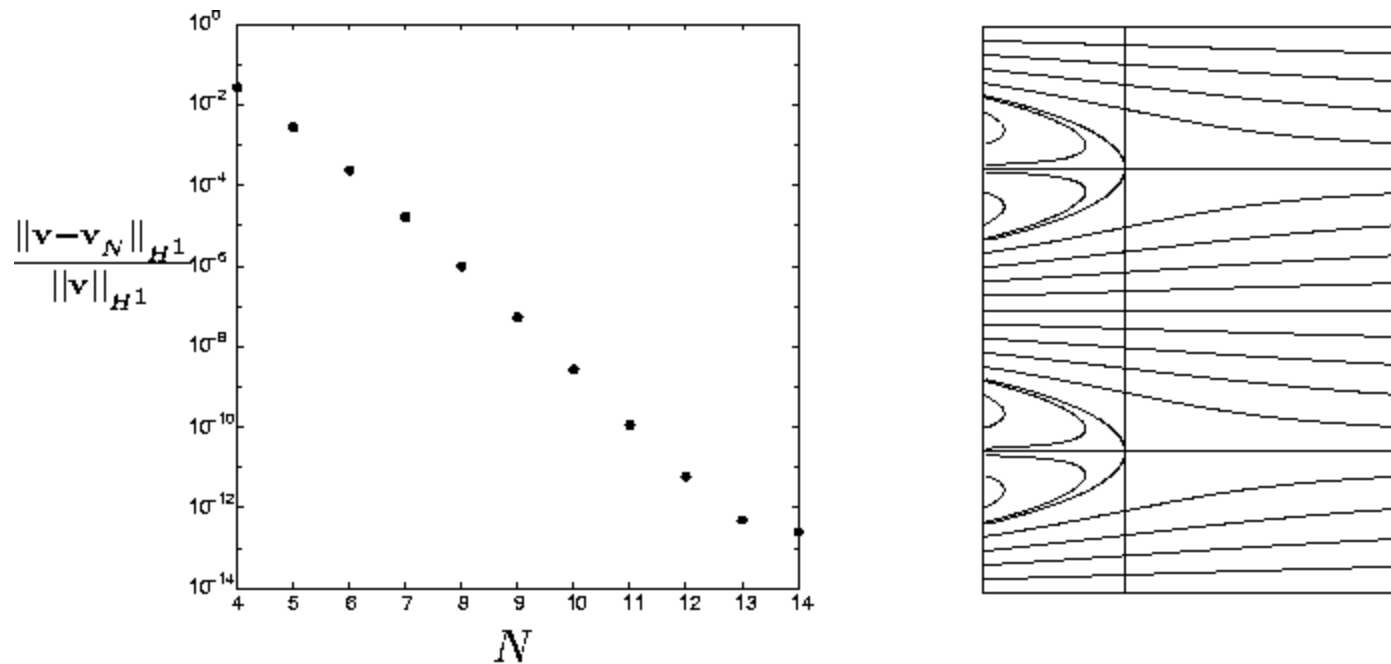
$E=3, N=4$

Accuracy

+

Costs

Spectral Element Convergence: Exponential with N



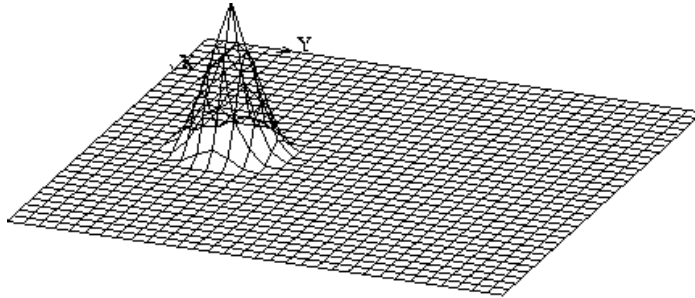
*Exact Navier-Stokes
solution due to
Kovazsnay(1948):*

$$v_x = 1 - e^{\lambda x} \cos 2\pi y$$

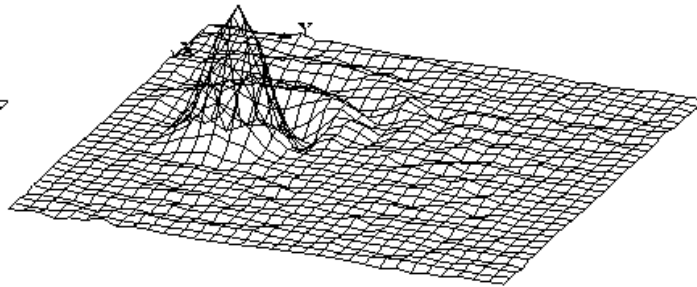
$$v_y = \frac{\lambda}{2\pi} e^{\lambda x} \sin 2\pi y$$

$$\lambda := \frac{Re}{2} - \sqrt{\frac{Re^2}{4} + 4\pi^2}$$

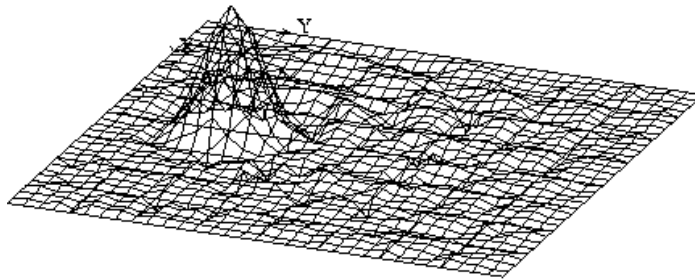
Excellent transport properties, even for *non-smooth* solutions



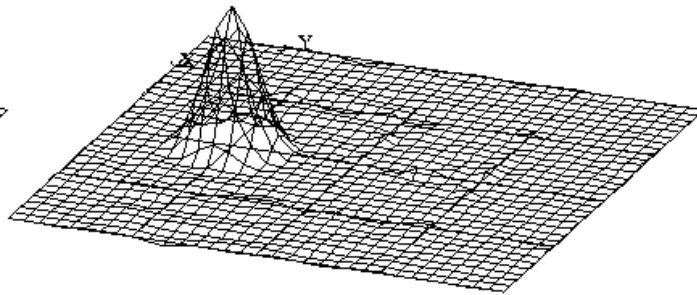
Initial Condition



$K_1 = 16, N = 2$



$K_1 = 8, N = 4$

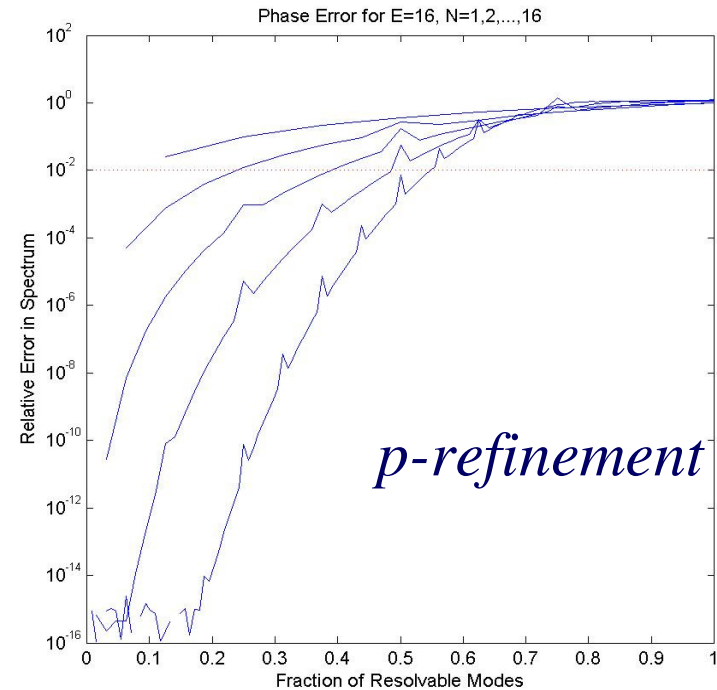
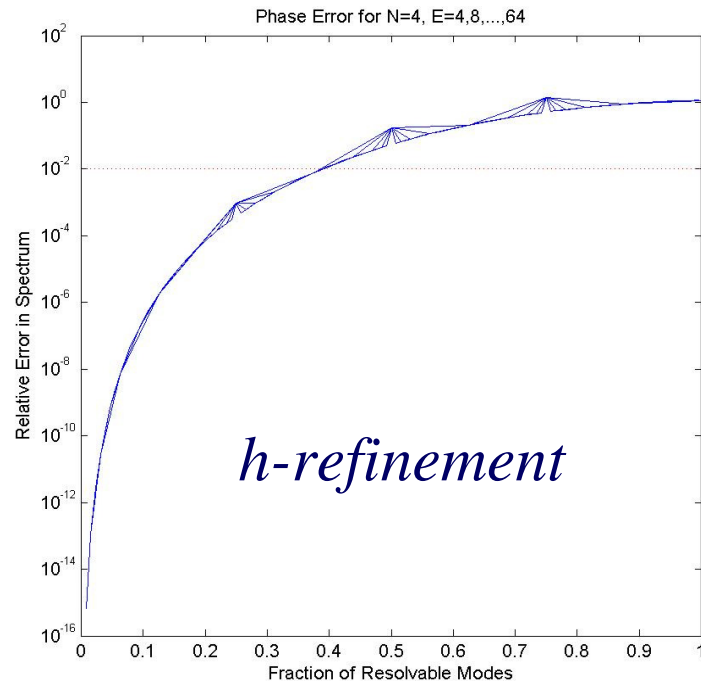


$K_1 = 4, N = 8$

Convection of non-smooth data on a 32x32 grid ($K_1 \times K_1$ spectral elements of order N).

(cf. Gottlieb & Orszag 77)

Relative Phase Error for h vs. p Refinement: $u_t + u_x = 0$



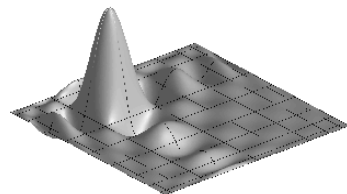
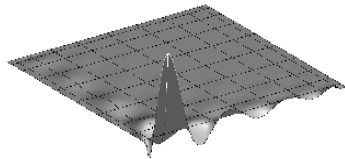
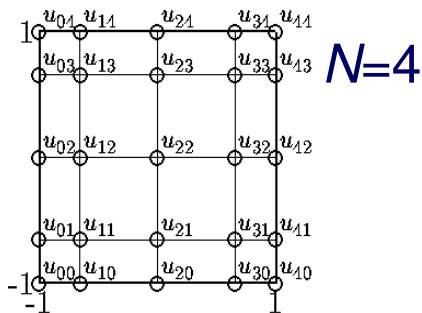
- ❑ X -axis = k / k_{max} , $k_{max} := n / 2$ (Nyquist)
- ❑ Fraction of resolvable modes increased only through p -refinement
- ❑ Diagonal mass matrix (low N significantly improved w/ full mass matrix)
- ❑ Polynomial approaches saturate at $k / k_{max} = 2 / \pi$

→ $N = 8-16 \sim$ point of marginal return

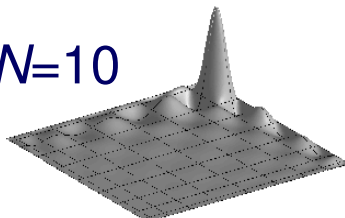
Costs

- ❑ Cost dominated by iterative solver costs, *proportional to*

- ❑ iteration count
- ❑ matrix-vector product + preconditioner cost



$N=10$



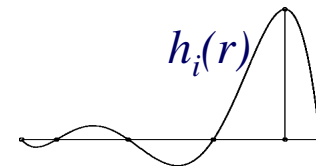
- ❑ Locally-structured tensor-product forms:

- ❑ minimal indirect addressing
- ❑ fast matrix-free operator evaluation
- ❑ fast local operator inversion via fast diagonalization method (FDM)
(*Approximate, when element deformed.*)

Matrix-Matrix Based Derivative Evaluation

□ *Local tensor-product form (2D),*

$$u(r, s) = \sum_{i=0}^N \sum_{j=0}^N u_{ij} h_i(r) h_j(s), \quad h_i(\xi_p) = \delta_{ip}, \quad h_i \in \mathbb{P}_N$$



allows derivatives to be evaluated as matrix-matrix products:

$$\frac{\partial u}{\partial r} \Big|_{\xi_i, \xi_j} = \sum_{p=0}^N u_{pj} \frac{dh_p}{dr} \Big|_{\xi_i} = \sum_p \underbrace{\hat{D}_{ip} u_{pj}}_{m \times m} =: D_r \underline{u}$$

Local “Matrix-Free” Stiffness Matrix in 3D

- For a deformed spectral element, Ω^k ,

$$A^k \underline{u}^k = \begin{pmatrix} D_r \\ D_s \\ D_t \end{pmatrix}^T \begin{pmatrix} G_{rr} & G_{rs} & G_{rt} \\ G_{rs} & G_{ss} & G_{st} \\ G_{rt} & G_{st} & G_{tt} \end{pmatrix} \begin{pmatrix} D_r \\ D_s \\ D_t \end{pmatrix} \underline{u}^k$$

$$D_r = (I \otimes I \otimes \hat{D}) \quad G_{rs} = J \circ B \circ \left(\frac{\partial r}{\partial x} \frac{\partial s}{\partial x} + \frac{\partial r}{\partial y} \frac{\partial s}{\partial y} + \frac{\partial r}{\partial z} \frac{\partial s}{\partial z} \right)$$

- Operation count is only $O(N^4)$ not $O(N^6)$ [Orszag '80]
- Memory access is 7 x number of points (G_{rr}, G_{rs} , etc., are *diagonal*)
- Work is dominated by matrix-matrix products involving D_r, D_s , etc.

Summary: Computational Efficiency

- ❑ Error decays exponentially with N , *typical* $N \sim 5-15$

- ❑ For $n=EN^3$ gridpoints, require
 - ❑ $O(n)$ memory accesses
 - ❑ $O(nN)$ work in the form of matrix-matrix products

- ❑ Standard p-type implementation gives
 - ❑ $O(nN^3)$ memory accesses
 - ❑ $O(nN^3)$ work in the form of matrix-vector products

- ❑ Extensions to high-order tets:
 - ❑ Karniadakis & Sherwin (tensor-product quadrature)
 - ❑ Hesthaven & Warburton (geometry/canonical factorization: $\mathbf{D}_r^T \mathbf{G}^e \mathbf{D}_r$)
 - ❑ Schoeberl et al. (orthogonal bases for linear operators)

Stability

Stabilizing High-Order Methods

In the absence of eddy viscosity, some type of stabilization is generally required at high Reynolds numbers.

Some options:

- ❑ high-order upwinding (e.g., DG, WENO)
- ❑ bubble functions
- ❑ spectrally vanishing viscosity
- ❑ *filtering*
- ❑ *dealiasing*

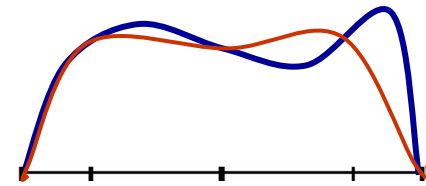
Filter-Based Stabilization

(Gottlieb et al., Don et al., Vandeveen, Boyd, ...)

□ At end of each time step:

- Interpolate u onto GLL points for P_{N-1}
- Interpolate back to GLL points for P_N

$$F_1(u) = I_{N-1} u$$



□ Results are smoother with linear combination:

(F. & Mullen 01)

$$F_\alpha(u) = (1-\alpha) u + \alpha I_{N-1} u \quad (\alpha \sim 0.05 - 0.2)$$

□ Post-processing — no change to existing solvers

□ Preserves interelement continuity and spectral accuracy

□ Equivalent to multiplying by $(1-\alpha)$ the N th coefficient in the expansion

$$\square u(x) = \sum u_k \phi_k(x) \quad \rightarrow \quad u^*(x) = \sum \sigma_k u_k \phi_k(x), \quad \sigma_k = 1, \quad \sigma_N = (1-\alpha)$$

$$\square \phi_k(x) := L_k(x) - L_{k-2}(x) \quad \text{(Boyd 98)}$$

Numerical Stability Test: Shear Layer Roll-Up

(Bell et al. JCP 89, Brown & Minion, JCP 95, F. & Mullen, CRAS 2001)

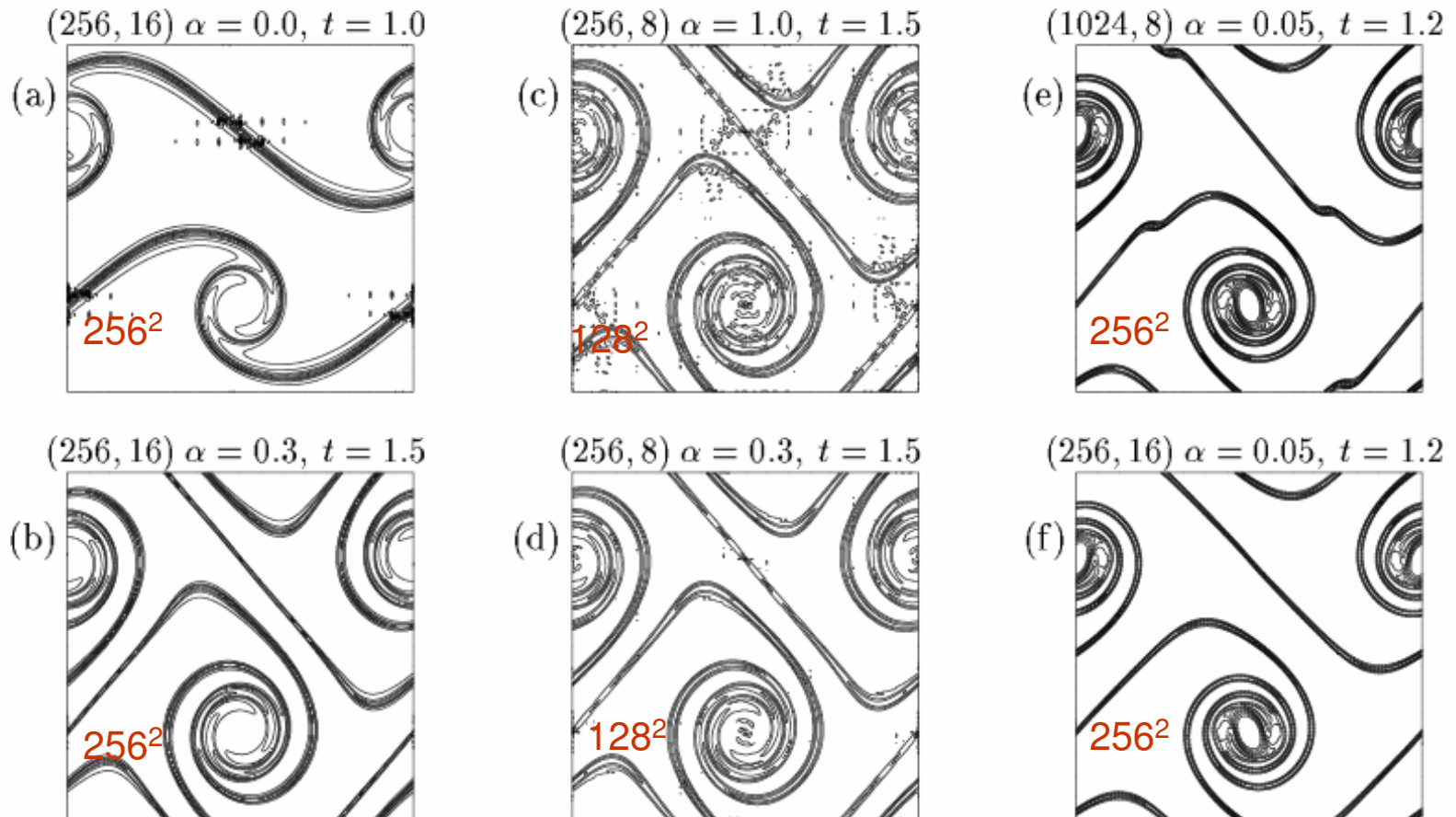


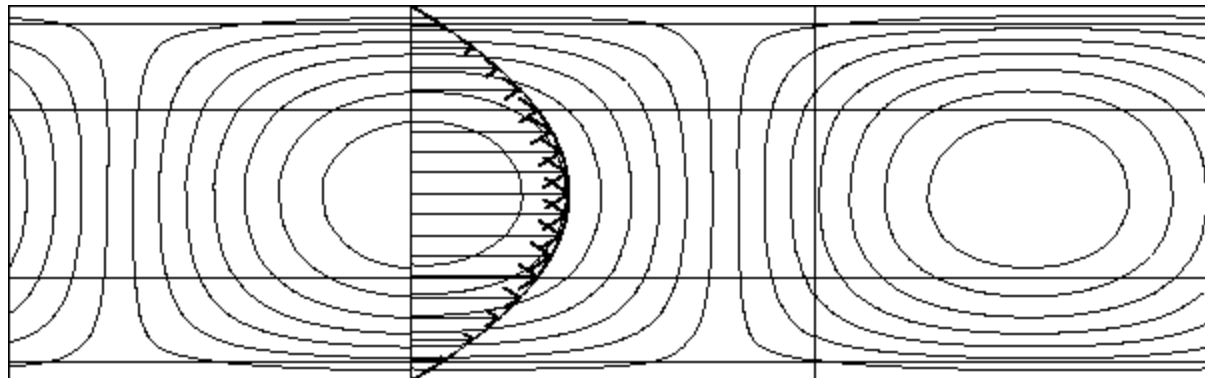
Figure 1: Vorticity for different (K, N) pairings: (a-d) $\rho = 30$, $Re = 10^5$, contours from -70 to 70 by 140/15; (e-f) $\rho = 100$, $Re = 40,000$, contours from -36 to 36 by 72/13. (cf. Fig. 3c in [4]).

Error in Predicted Growth Rate for Orr-Sommerfeld Problem at $Re=7500$

(Malik & Zang 84)

Spatial and Temporal Convergence (FM, 2001)

N	$\Delta t = 0.003125$		$N = 17$	2nd Order		3rd Order	
	$\alpha = 0.0$	$\alpha = 0.2$		Δt	$\alpha = 0.0$	$\alpha = 0.2$	$\alpha = 0.0$
7	0.23641	0.27450	0.20000	0.12621	0.12621	171.370	0.02066
9	0.00173	0.11929	0.10000	0.03465	0.03465	0.00267	0.00268
11	0.00455	0.01114	0.05000	0.00910	0.00911	161.134	0.00040
13	0.00004	0.00074	0.02500	0.00238	0.00238	1.04463	0.00012
15	0.00010	0.00017	0.01250	0.00065	0.00066	0.00008	0.00008



Base velocity profile and perturbation streamlines

Filtering permits $Re_{\delta_{99}} > 700$ for transitional boundary layer calculations

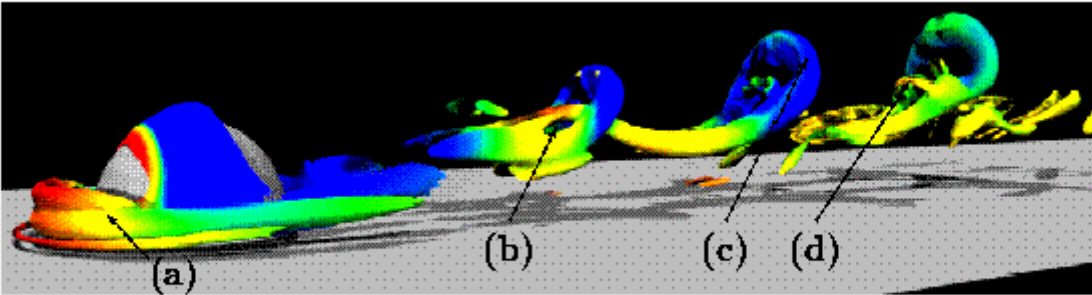
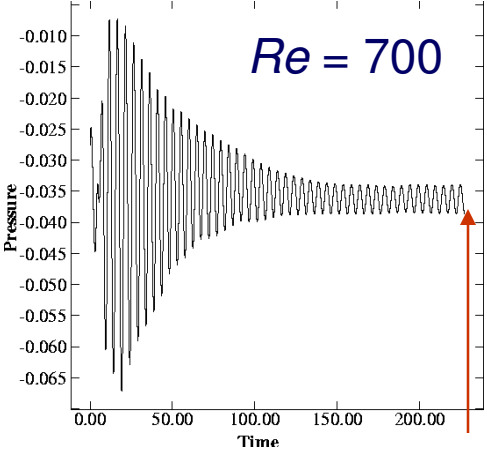
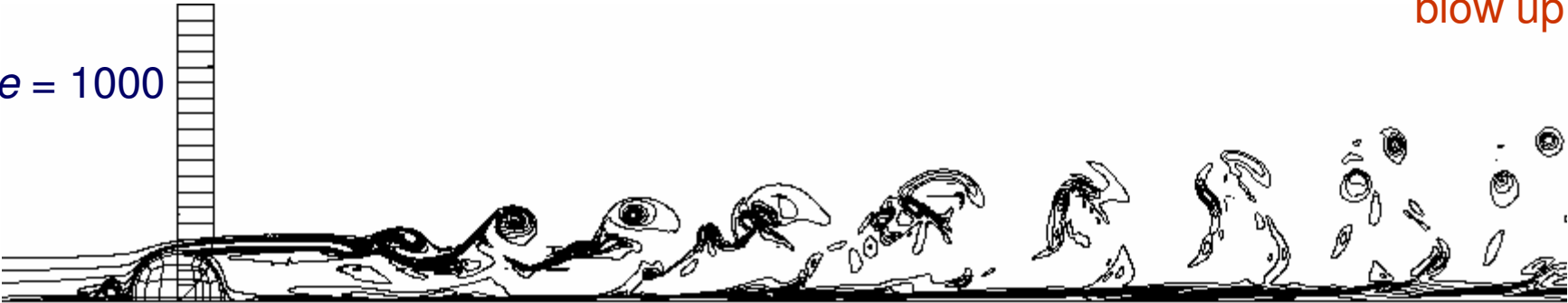


Figure 1: Principal vortex structures identified by $\lambda_2 = -1$ isosurfaces at $Re_* = 760$: standing horseshoe vortex (a), interlaced tails (b), hairpin head (c), and bridge (d). Colors indicate pressure. ($K=1021, N = 15$).



blow up

$Re = 1000$



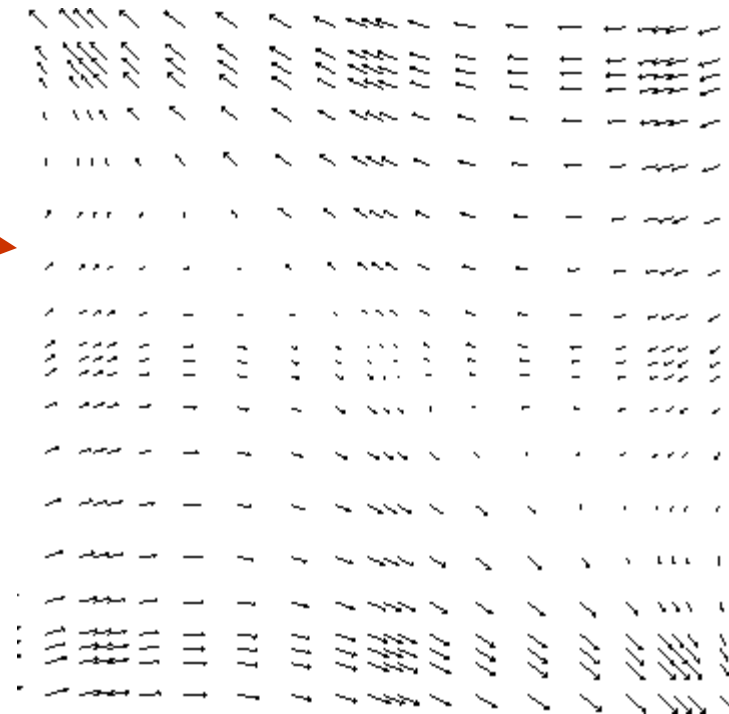
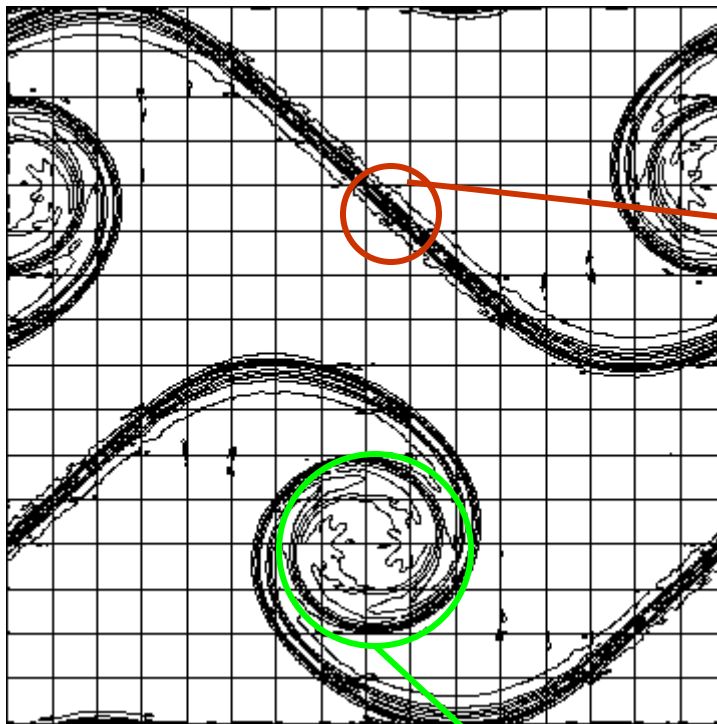
$Re = 3500$



Why Does Filtering Work ?

(Or, Why Do the Unfiltered Equations Fail?)

Double shear layer example:



Ok

*High-strain regions
are troublesome...*

Why Does Filtering Work ?

(Or, Why Do the Unfiltered Equations Fail?)

Consider the model problem: $\frac{\partial u}{\partial t} = -\mathbf{c} \cdot \nabla u$

Weighted residual formulation: $B \frac{du}{dt} = -C \underline{u}$

$$B_{ij} = \int_{\Omega} \phi_i \phi_j dV = \text{symm. pos. def.}$$

$$\begin{aligned} C_{ij} &= \int_{\Omega} \phi_i \mathbf{c} \cdot \nabla \phi_j dV \\ &= - \int_{\Omega} \phi_j \mathbf{c} \cdot \nabla \phi_i dV - \int_{\Omega} \phi_j \phi_j \nabla \cdot \mathbf{c} dV \\ &= \text{skew symmetric, if } \nabla \cdot \mathbf{c} \equiv 0. \end{aligned}$$

$B^{-1}C$ imaginary eigenvalues

Discrete problem should never blow up.

Why Does Filtering Work ?

(*Or, Why Do the Unfiltered Equations Fail?*)

Weighted residual formulation vs. spectral element method:

$$C_{ij} = (\phi_i, \mathbf{c} \cdot \nabla \phi_j) = -C_{ji}$$

$$\tilde{C}_{ij} = (\phi_i, \mathbf{c} \cdot \nabla \phi_j)_N \neq -\tilde{C}_{ji}$$

This suggests the use of over-integration (dealiasing) to ensure that skew-symmetry is retained

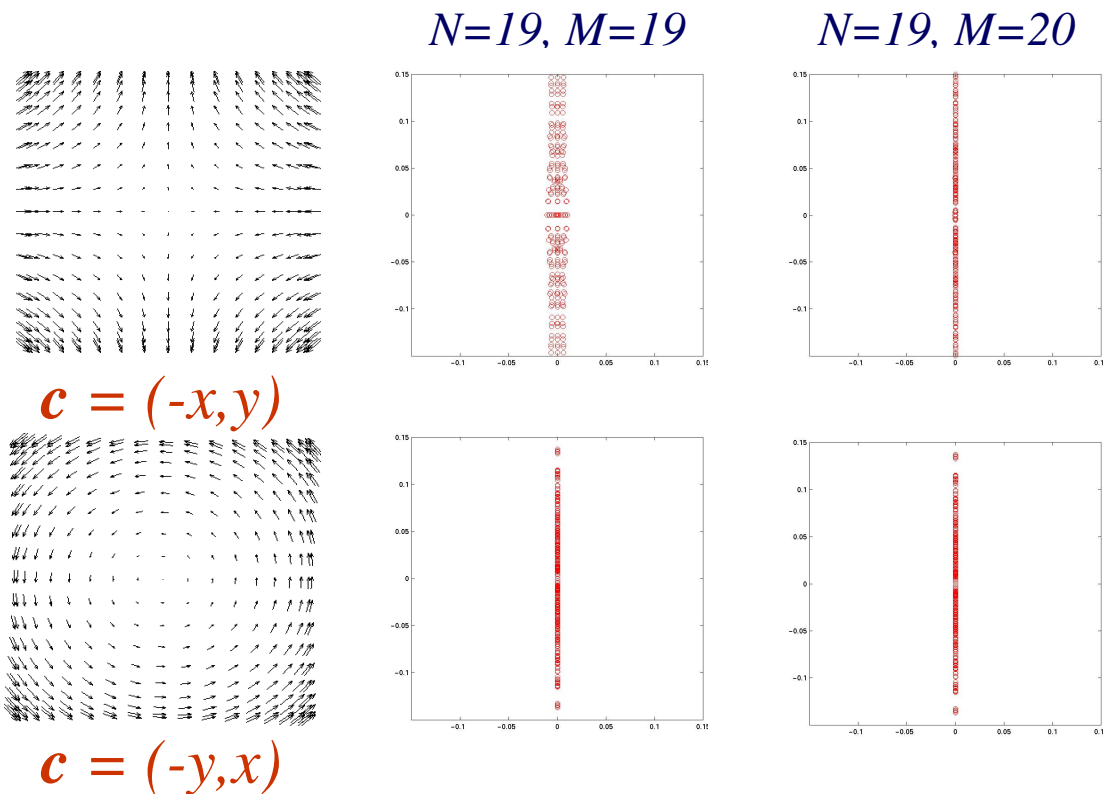
$$C_{ij} = (J\phi_i, (J\mathbf{c}) \cdot J\nabla\phi_j)_M$$

$$J_{pq} := h_q^N(\xi_p^M) \quad \text{interpolation matrix (1D, single element)}$$

(Orszag '72, Kirby & Karniadakis '03, Kirby & Sherwin '06)

Aliased / Dealiased Eigenvalues: $u_t + \mathbf{c} \cdot \nabla u = 0$

- ❑ Velocity fields model first-order terms in expansion of straining and rotating flows.
 - ❑ For straining case, $\frac{d}{dt}|u|^2 \sim |\hat{u}_{N+1}|^2 - |\hat{u}_{N+1}|^2$
 - ❑ Rotational case is skew-symmetric.
 - ❑ Filtering attacks the leading-order unstable mode.

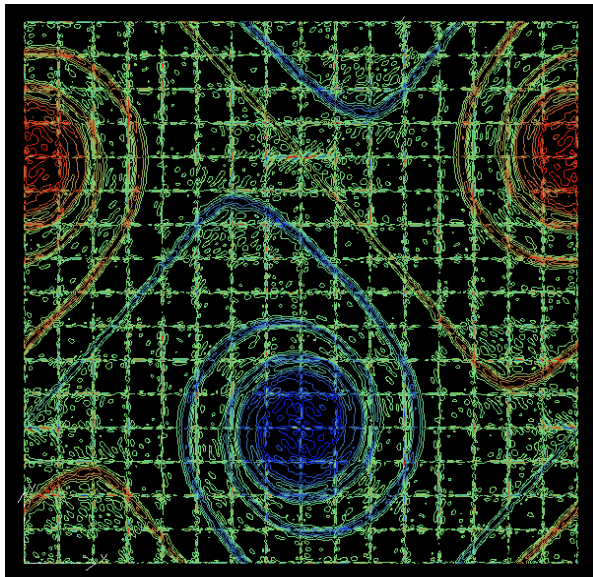


Stabilization Summary

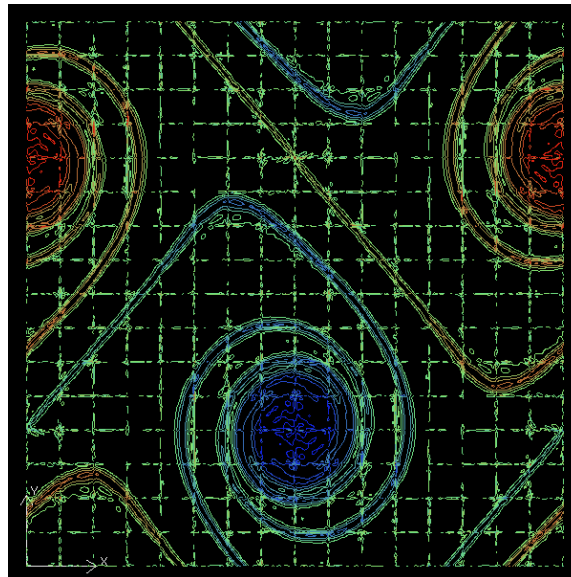
- ❑ Filtering acts like well-tuned hyperviscosity
 - ❑ Attacks only the fine scale modes (that, numerically speaking, shouldn't have energy anyway...)
 - ❑ Can precisely identify which modes in the SE expansion to suppress (unlike differential filters)
 - ❑ Does not compromise spectral convergence
- ❑ Dealiasing of convection operator recommended for high Reynolds number applications to avoid spurious eigenvalues
 - ❑ Can run double shear-layer roll-up problem *forever* with
 - $\nu = 0$,
 - *no filtering*

Dealiased Shear Layer Roll-Up Problem, 128^2

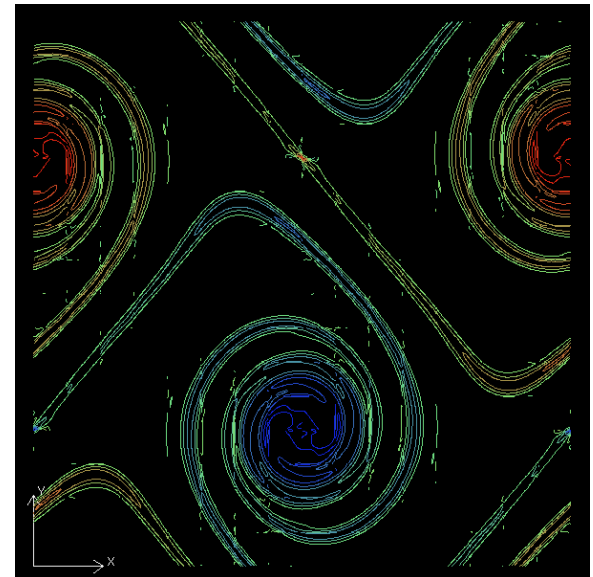
$\nu = 0$, no filter



$\nu = 10^{-5}$, no filter



$\nu = 0$, filter = (.1,.025)



Linear Solvers

Linear Solvers for Incompressible Navier-Stokes

- Navier-Stokes time advancement:

$$\frac{\partial \vec{u}}{\partial t} + \vec{u} \cdot \nabla \vec{u} = -\nabla P + \frac{1}{Re} \nabla^2 \vec{u}$$

$$-\nabla \cdot \vec{u} = 0$$

- Nonlinear term: *explicit*

- k th-order backward difference formula / extrapolation
- characteristics (Pironneau '82, MPR '90)

- Stokes problem: pressure/viscous decoupling:

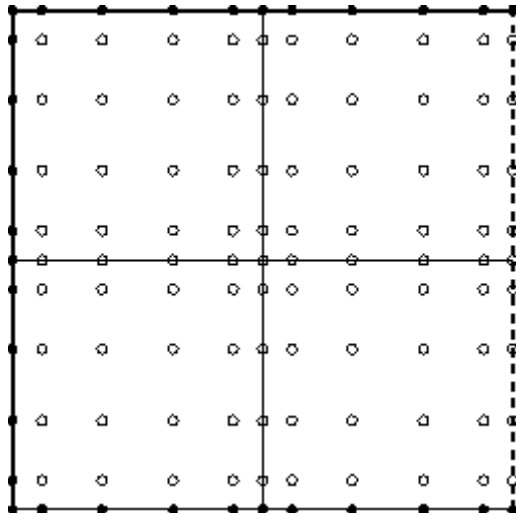
- 3 Helmholtz solves for velocity (*“easy” w/ Jacobi-precond. CG*)
- (consistent) Poisson equation for pressure (*computationally dominant*)

$P_N - P_{N-2}$ Spectral Element Method for Navier-Stokes (MP 89)

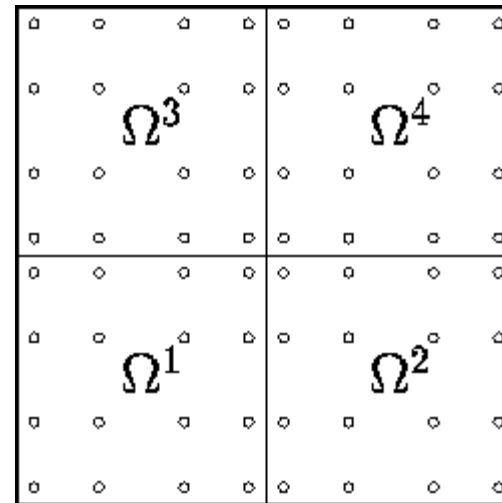
WRT: Find $\mathbf{u} \in X^N, p \in Y^N$ such that:

$$\begin{aligned} \frac{1}{Re} (\nabla \mathbf{u}, \nabla \mathbf{v})_{GL} + \frac{1}{\Delta t} (\mathbf{u}, \mathbf{v})_{GL} - (p, \nabla \cdot \mathbf{v})_G &= (\mathbf{f}, \mathbf{v})_{GL} \quad \forall \mathbf{v} \in X^N \subset H^1 \\ - (q, \nabla \cdot \mathbf{u})_G &= 0 \quad \forall q \in Y^N \subset L^2 \end{aligned}$$

Velocity, \mathbf{u} in P_N , continuous
 Pressure, p in P_{N-2} , discontinuous



Gauss-Lobatto Legendre points
(velocity)



Gauss Legendre points
(pressure)

Navier-Stokes Solution Strategy

- ❑ Semi-implicit: explicit treatment of nonlinear term.
- ❑ Leads to Stokes saddle problem, which is algebraically split

MPR 90, Blair-Perot 93, Couzy 95

$$\begin{bmatrix} \mathbf{H} & -\mathbf{D}^T \\ -\mathbf{D} & 0 \end{bmatrix} \begin{pmatrix} \underline{\mathbf{u}}^n \\ \underline{p}^n - \underline{p}^{n-1} \end{pmatrix} = \begin{pmatrix} \mathbf{B}\underline{\mathbf{f}} + \mathbf{D}^T \underline{p}^{n-1} \\ \underline{f}_p \end{pmatrix}$$

$$\begin{bmatrix} \mathbf{H} & -\frac{\Delta t}{\beta_0} \mathbf{H}\mathbf{B}^{-1}\mathbf{D}^T \\ \mathbf{0} & E \end{bmatrix} \begin{pmatrix} \underline{\mathbf{u}}^n \\ \underline{p}^n - \underline{p}^{n-1} \end{pmatrix} = \begin{pmatrix} \mathbf{B}\underline{\mathbf{f}} + \mathbf{D}^T \underline{p}^{n-1} \\ \underline{g} \end{pmatrix} + \begin{pmatrix} \underline{\mathbf{r}} \\ \underline{0} \end{pmatrix},$$

$$E := \frac{\Delta t}{\beta_0} \mathbf{D}\mathbf{B}^{-1}\mathbf{D}^T, \quad \underline{\mathbf{r}} = O(\Delta t^2)$$

- ❑ E - consistent Poisson operator for pressure, SPD
 - ❑ Stiffest substep in Navier-Stokes time advancement
 - ❑ Most compute-intensive phase
 - ❑ Spectrally equivalent to SEM Laplacian, \mathbf{A}

Pressure Solution Strategy: $E p^n = g^n$

1. Projection: compute best approximation from previous time steps

- ❑ Compute p^* in $\text{span}\{p^{n-1}, p^{n-2}, \dots, p^{n-l}\}$ through straightforward projection.
- ❑ Typically a 2-fold savings in Navier-Stokes solution time.
- ❑ Cost: 1 (or 2) matvecs in E per timestep

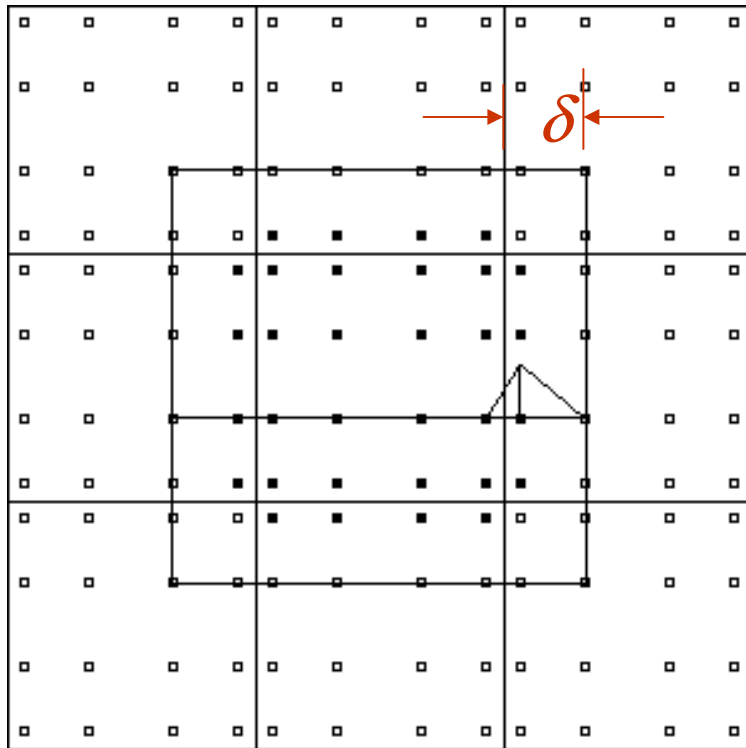
2. Preconditioned CG or GMRES to solve

$$E \Delta p = g^n - E p^*$$

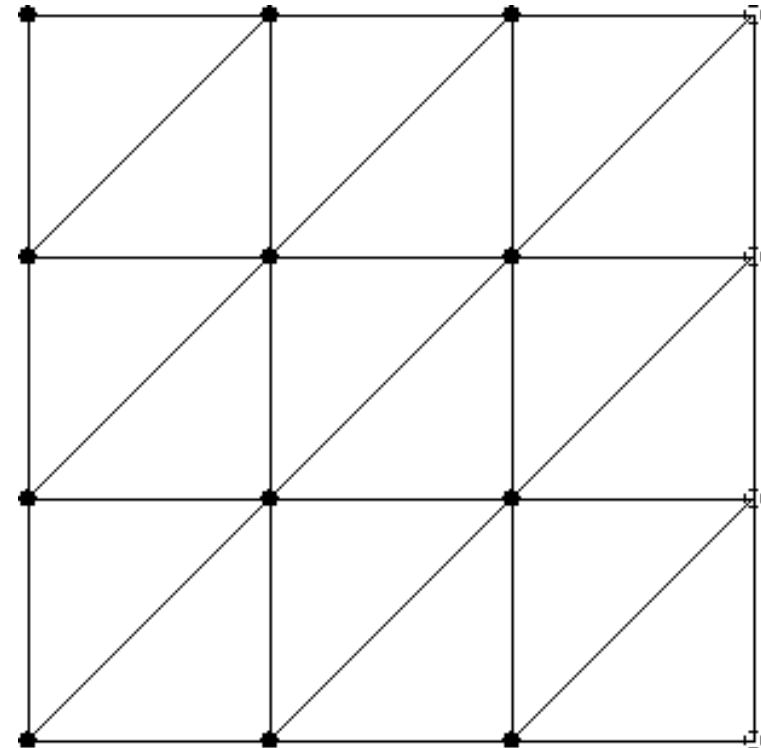
Two-Level Overlapping Additive Schwarz Preconditioner

(Dryja & Widlund 87, Pahl 93, PF 97, FMT 00)

$$\underline{z} = M\underline{r} = \sum_{e=1}^E R_e^T A_e^{-1} R_e \underline{r} + R_0^T A_0^{-1} R_0 \underline{r}$$



Local Overlapping Solves: FEM-based Poisson problems with homogeneous Dirichlet boundary conditions, A_e .



Coarse Grid Solve: Poisson problem using linear finite elements on entire spectral element mesh, A_0 (GLOBAL).

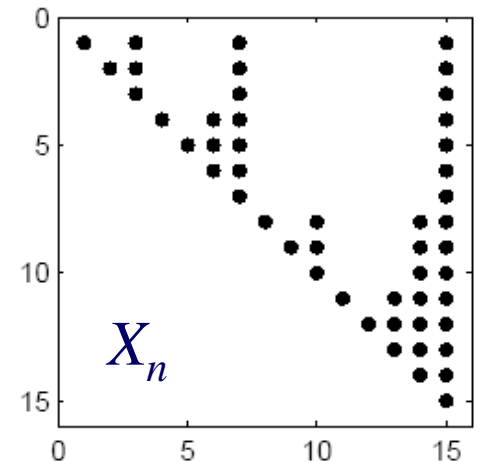
Solvers for Overlapping Schwarz / Multigrid

Local Solves: fast diagonalization method (Rice et al. '64, Couzy '95)

- ❑ $A_e^{-1} = (S \otimes S) (I \otimes \Lambda_x + \Lambda_y \otimes I)^{-1} (S \otimes S)^T$
- ❑ Complexity $< A p$
- ❑ For deformed case, approximate with nearest rectangular brick

Coarse Grid Solver: cast solution as projection onto A_0 -conjugate basis (PF '96, Tufo & F '01)

- ❑ $\underline{x}_0 = X_l X_l^T \underline{b}_0$
- ❑ Matrix-vector products inherently parallel
- ❑ Here, choose basis $X_l = (\underline{x}_1, \underline{x}_2, \dots, \underline{x}_l)$ to be *sparse*.
- ❑ Use Gram-Schmidt to fill remainder of X_l as $l \rightarrow n$
- ❑ Properly ordered, $X_n X_n^T = A_0^{-1}$ is a quasi-sparse factorization of A_0^{-1}
- ❑ *Sublinear in P , minimal number of messages.*

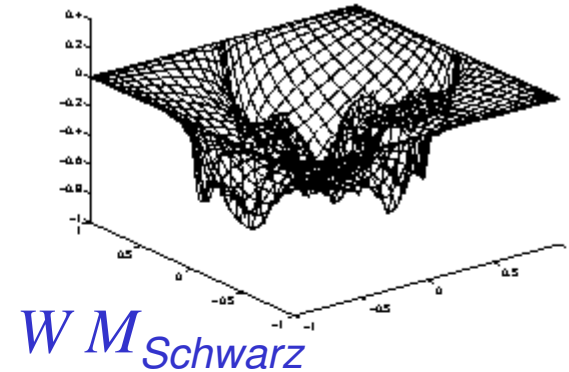
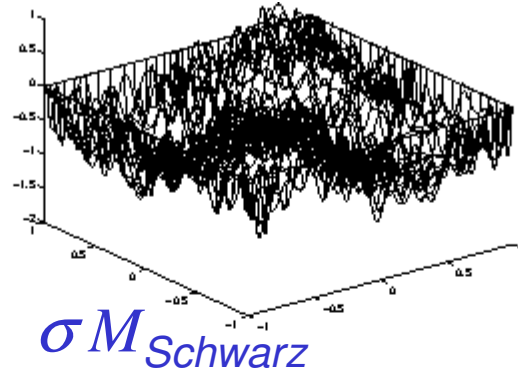
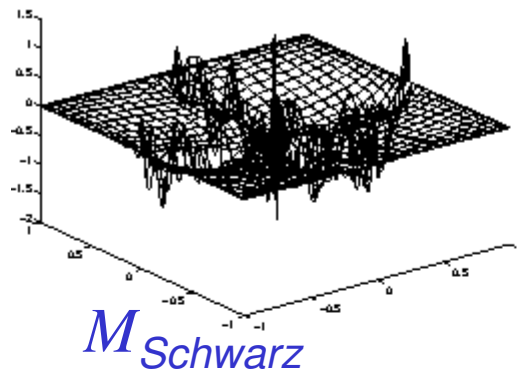


Two-Level Schwarz Heuristics

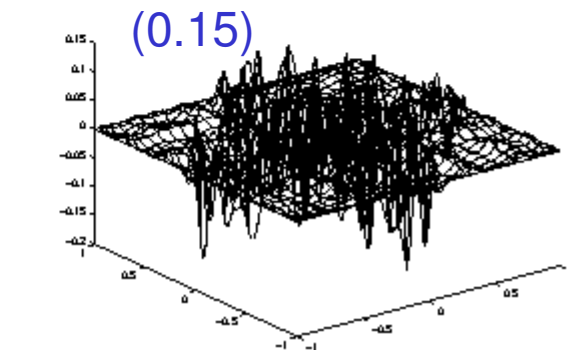
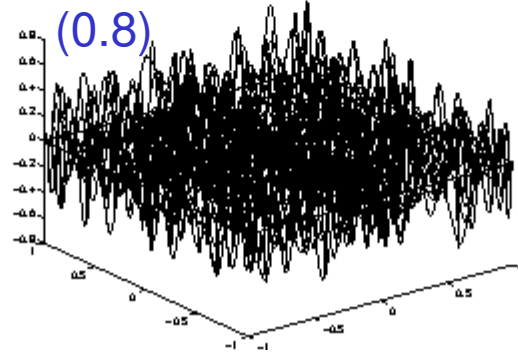
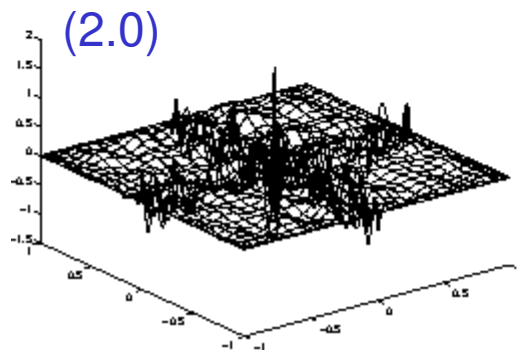
- ❑ Local solves eliminate fine-scale error.
- ❑ Remaining error, due to Green's functions from incorrect BCs on the local solves, is at scale $O(H)$, which is corrected by the coarse-grid solve.
- ❑ Additive preconditioning works in CG / GMRES contexts because eigenvalues of (preconditioned) fine and coarse modes are pushed towards unity.

Importance of weighting by W : Poisson eqn. example

❑ Error after a single Schwarz smoothing step



❑ Error after coarse-grid correction

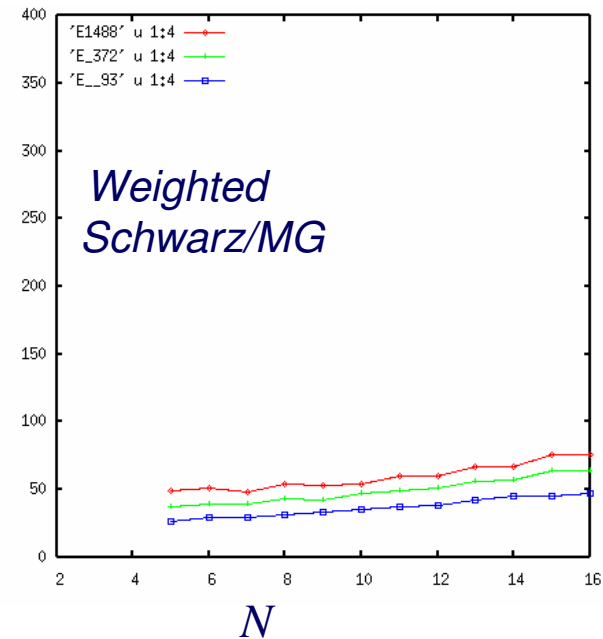
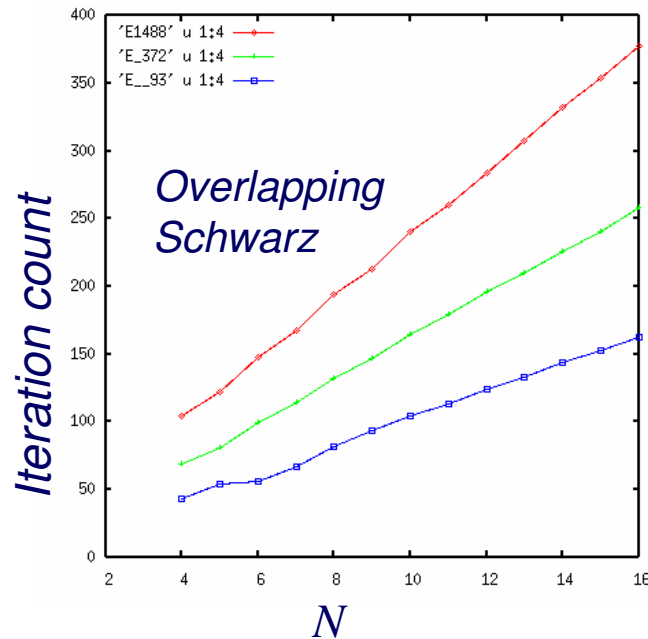
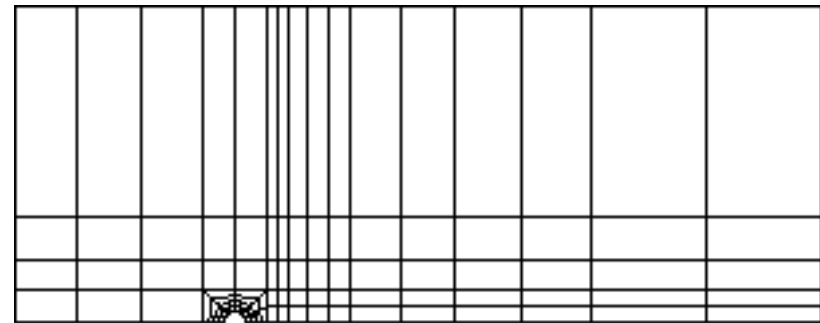


❑ *Weighting the additive-Schwarz step is essential to ensuring a smooth error*
(Szyld has recent results)

E -Based Schwarz vs. SEMG for *High-Aspect Ratio* Elements

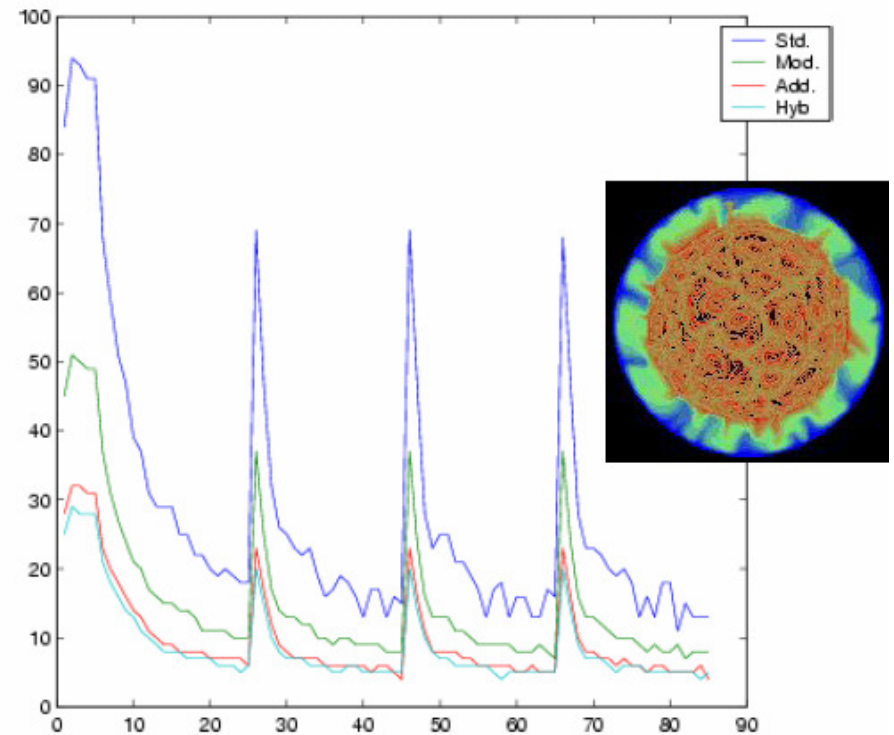
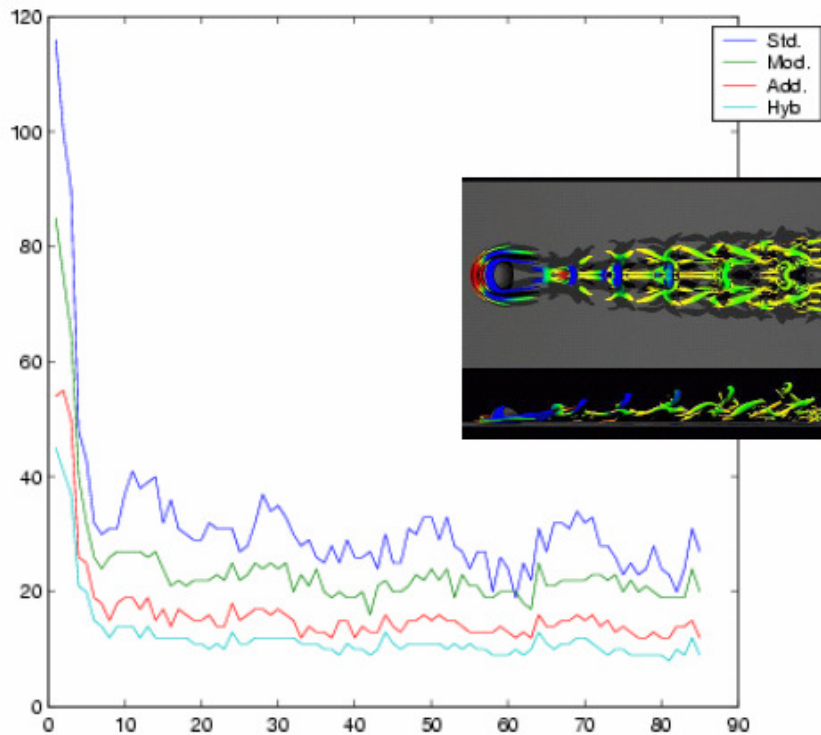
- Base mesh of $E=93$ elements
 - Quad refine to generate $E=372$ and $E=1488$ elements,
 - $N=4, \dots, 16$
 - SEMG reduces E and N dependence
 - **2.5 X reduction** in Navier-Stokes CPU time for $N=16$

2D Navier-Stokes Model Problem



Iteration Histories for 3D Unsteady Navier-Stokes ($n \sim 10^6$)

- Std. — 2-level additive Schwarz $R_e^T A_e R_e$
- Mod. — 2-level additive Schwarz, based on $WR_e^T E_e R_e$
- Add. — 3-level additive scheme
- Hyb. — 3-level multiplicative scheme



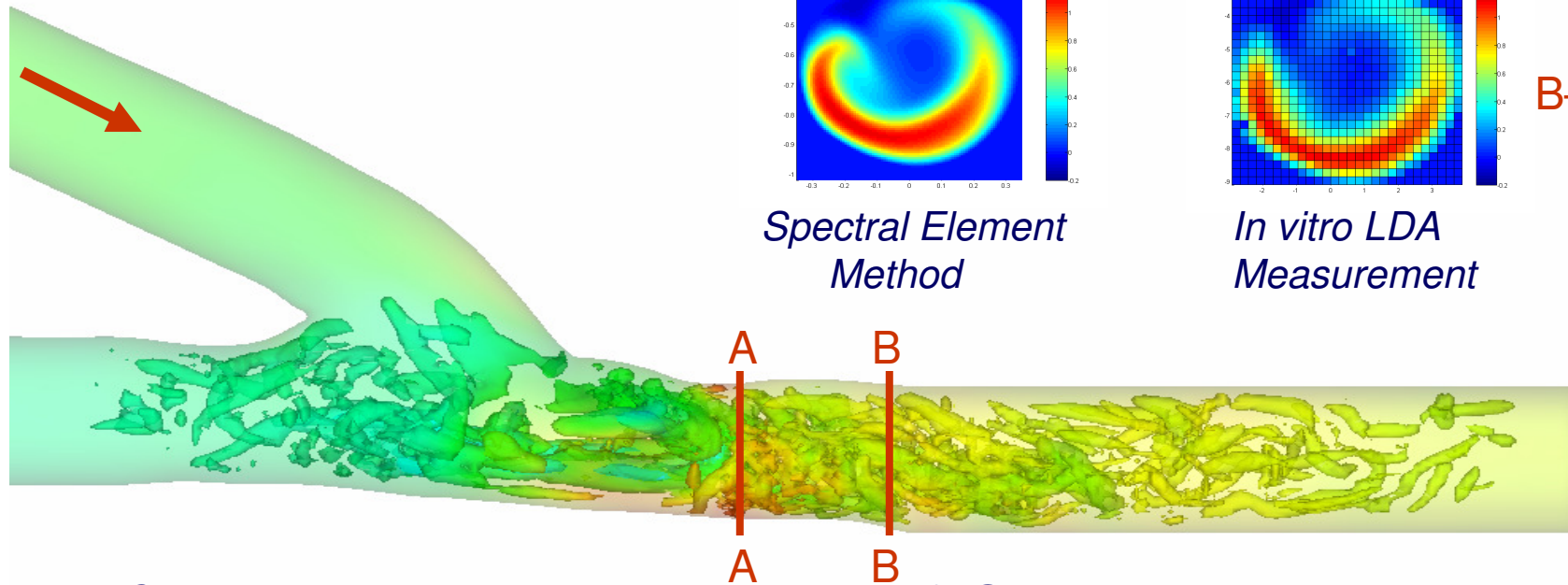
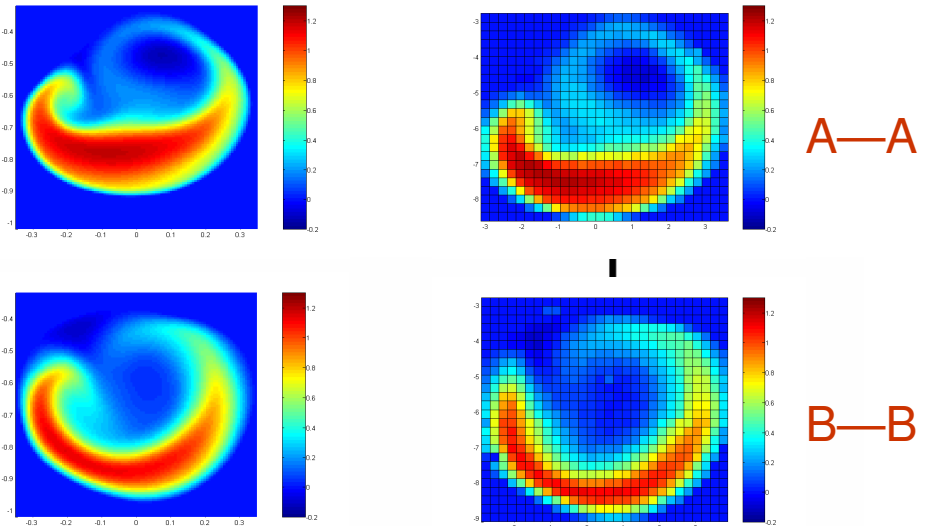
SEM Examples

Transition in Vascular Flows

w/ F. Loth, UIC

Comparison of spectral element and measured velocity distributions in an arteriovenous graft, $Re_G=1200$

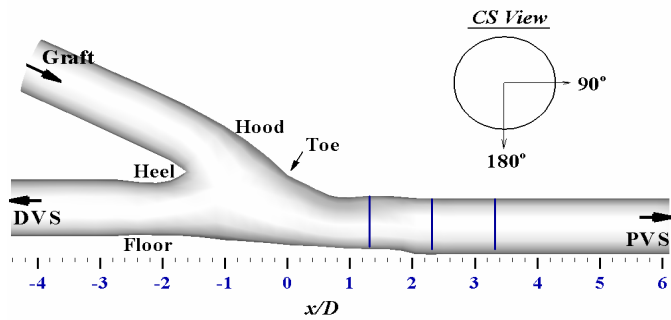
Mean Axial Velocity



Coherent structures in arteriovenous graft @ $Re_G = 1200$

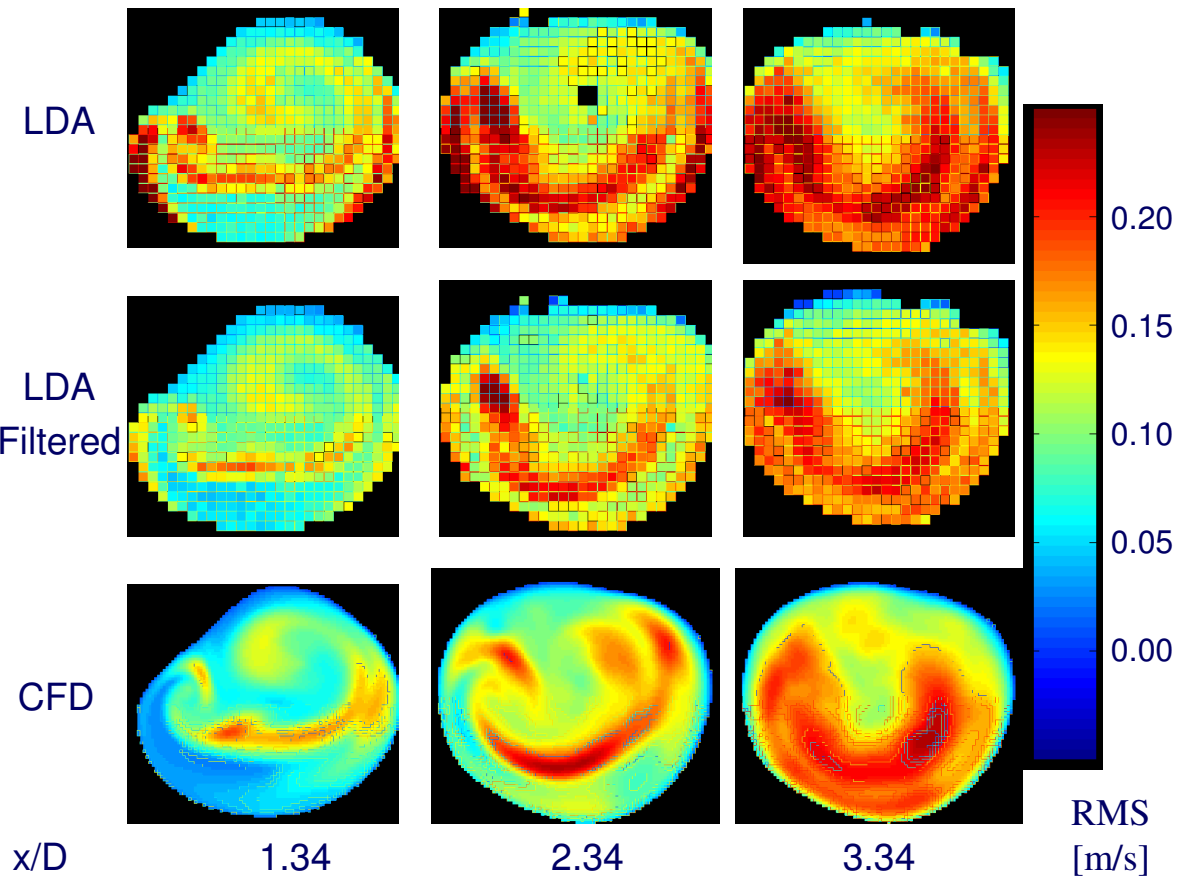
(Computations by S.W. Lee, UIC. Experiments by D. Smith, UIC)

RMS for Re 1200, 70:30 flow division

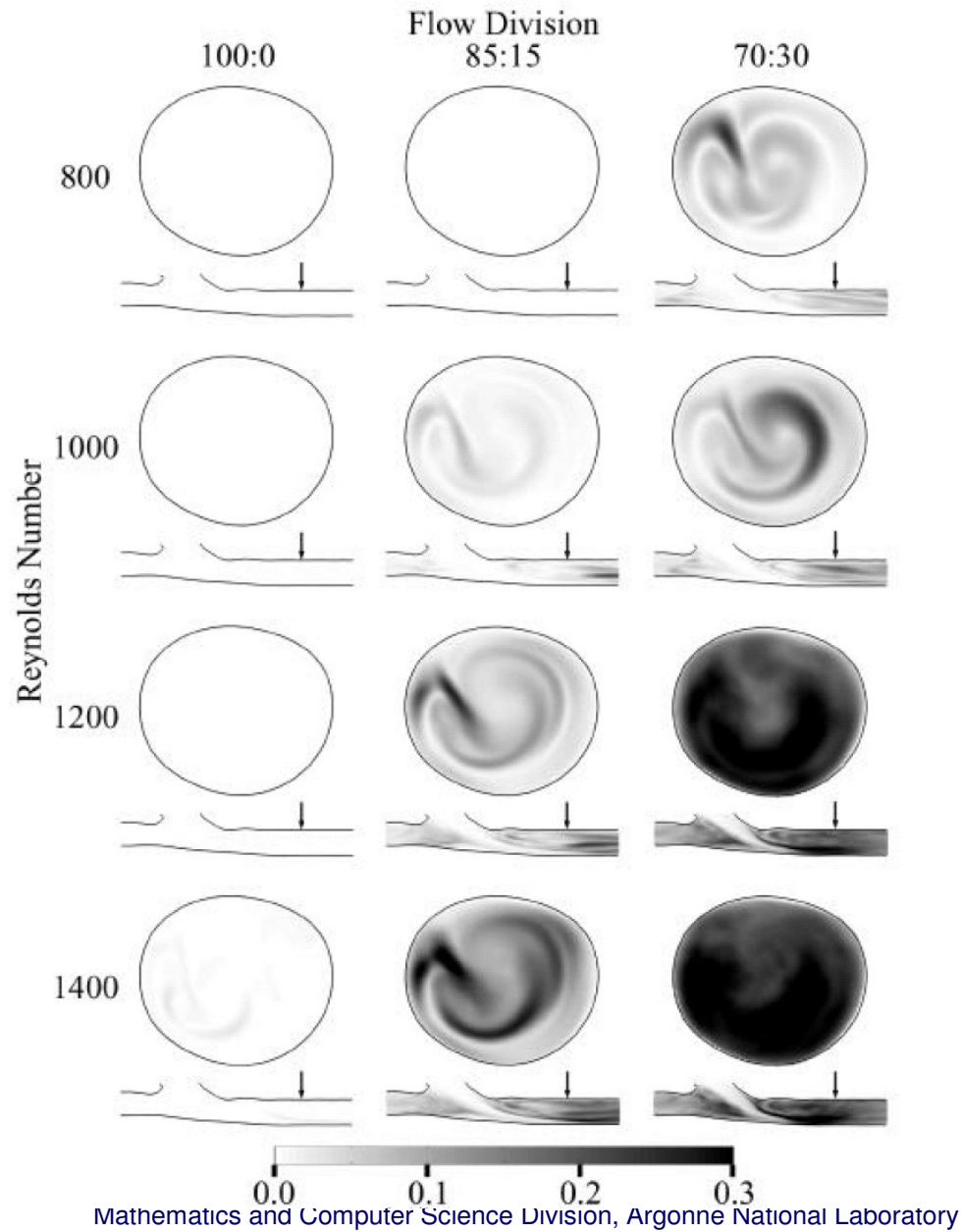


Fluctuation of Axial Velocity Component (RMS)

Experimental data is low-pass (< 250 Hz) filtered to remove spurious fluctuations inherent in LDA measurements of regions of high shear flow.

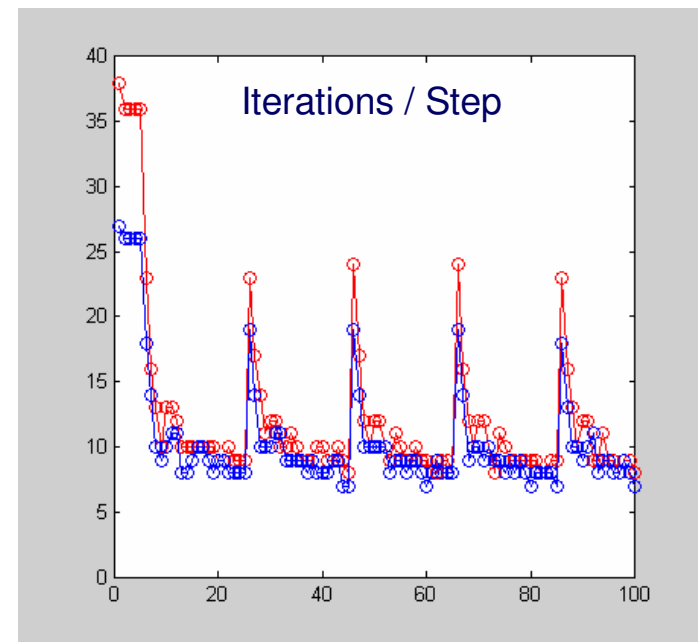
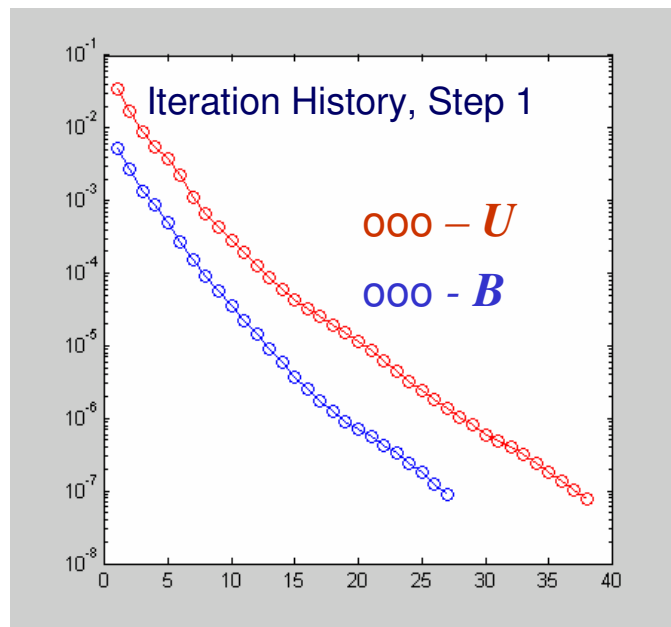
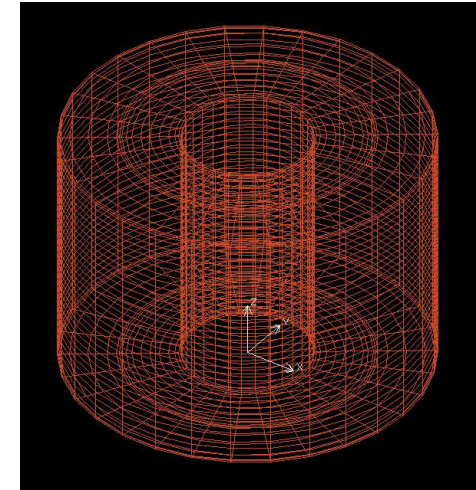


Influence of Reynolds Number and Flow Division on u_{rms}



SEMG Scalability: Incompressible MHD

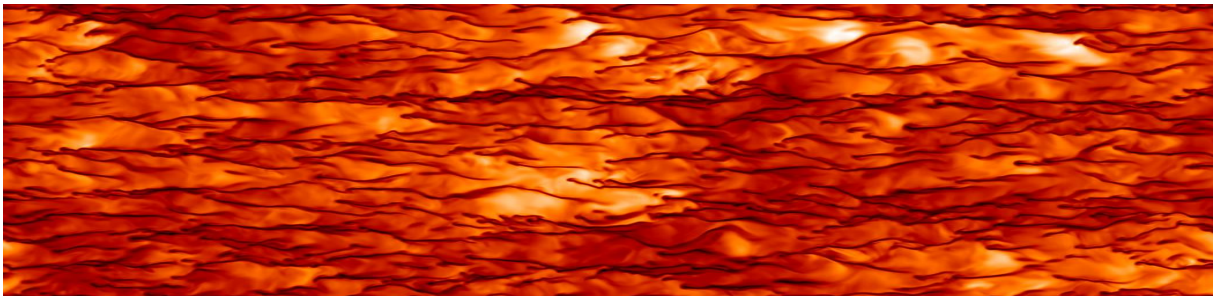
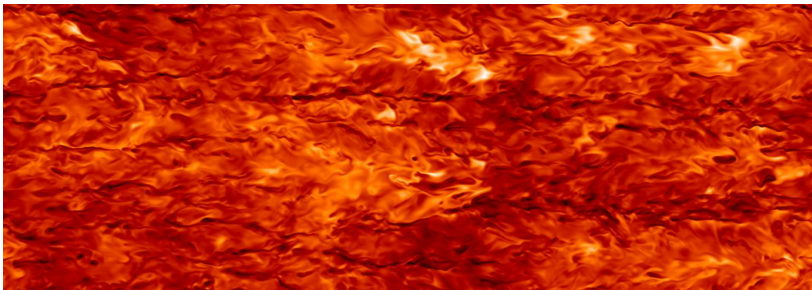
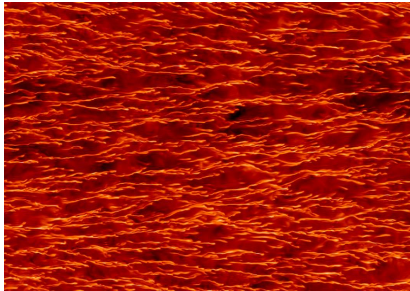
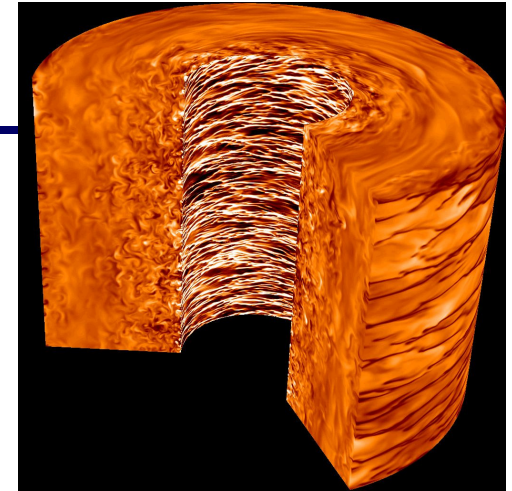
- ❑ Study of turbulent magneto-rotational instabilities (w/ F. Cattaneo & A. Obabko, UC)
- ❑ $E=97000, N=9$ ($n = 71 M$)
- ❑ $P=32768$
- ❑ $\sim .8 \text{ sec/step}$
- ❑ $\sim 8 \text{ iterations / step for } U \text{ \& } B$
- ❑ *Similar behavior for $n=112 M$*



Numerical Magneto-Rotational Instabilities

w/ Fausto Cattaneo (ANL/UC) and Aleks Obabko (UC)

- SEM discretization of incompressible MHD (112 M gridpoints)
- Hydrodynamically stable Taylor-Couette flow



• *Distributions of excess angular velocity at inner, mid, and outer radii*

• *Computations using 16K processors on BGW*

• ***Simulation Predicts:***

- ***MRI***

- ***sustained dynamo***

MRI Angular Velocity Perturbation ($\mathbf{v}' = \mathbf{v} - \langle \mathbf{v} \rangle$)

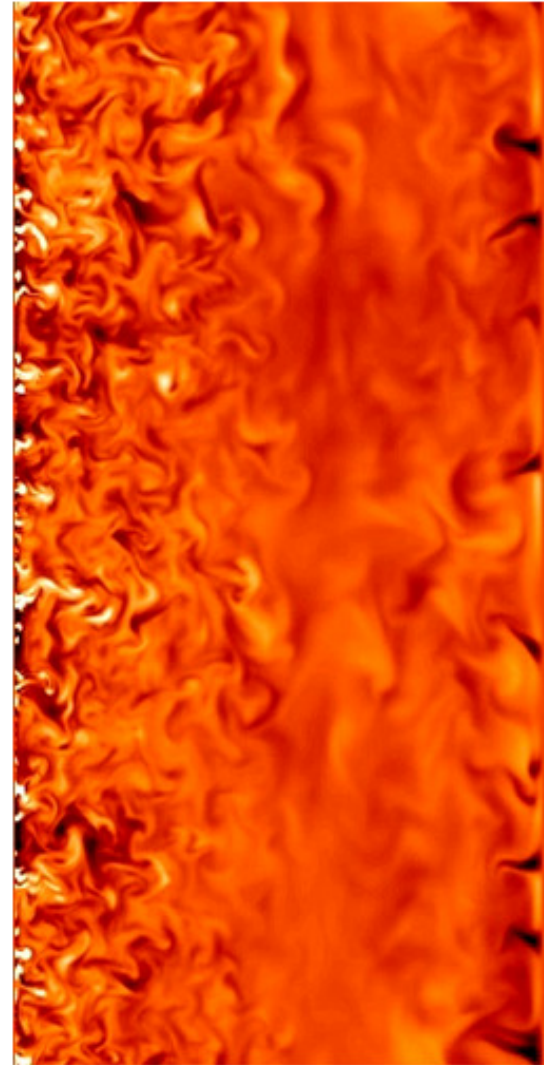
Axisymmetric

Inner Wall



Outer Wall

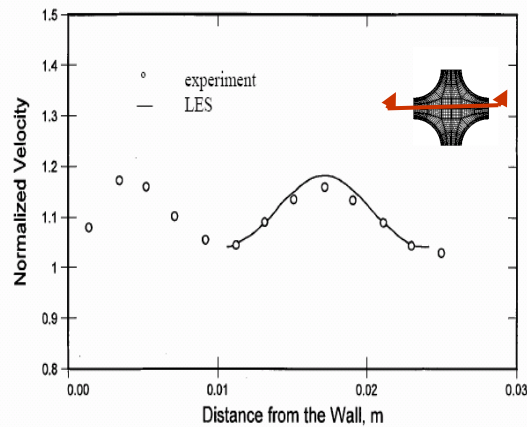
3D



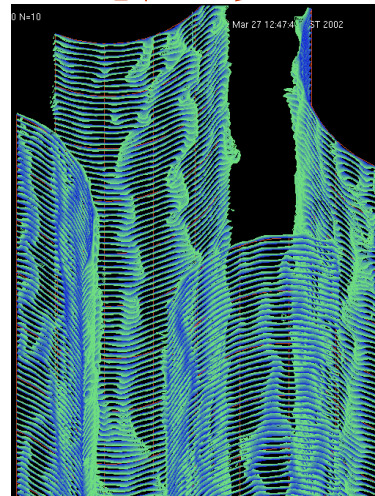
Rod Bundle Flow at $Re=30,000$

w/ C. Tzanos '05

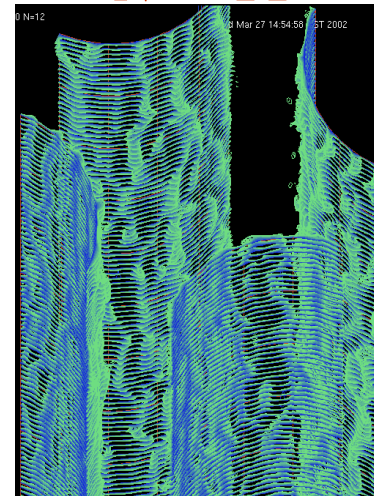
Low-speed streaks and log-law velocity profiles



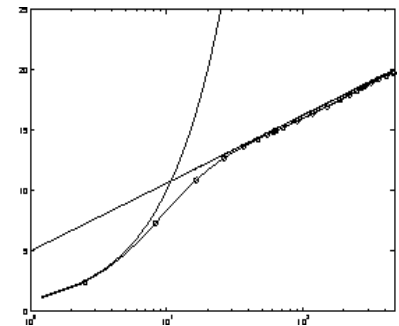
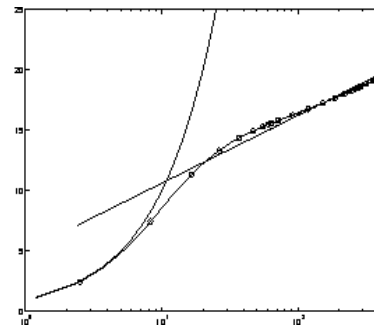
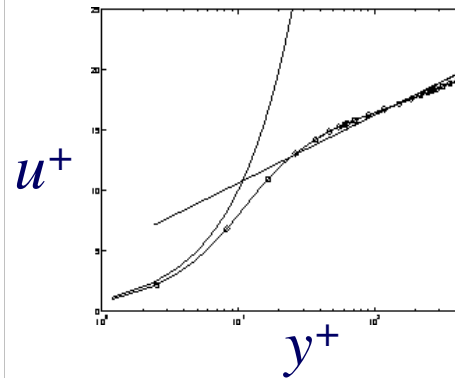
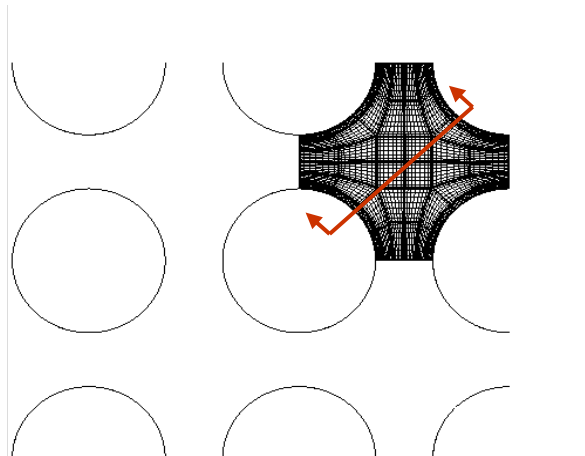
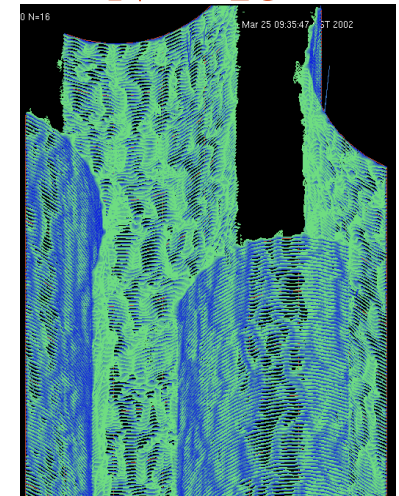
$N = 9$



$N = 11$

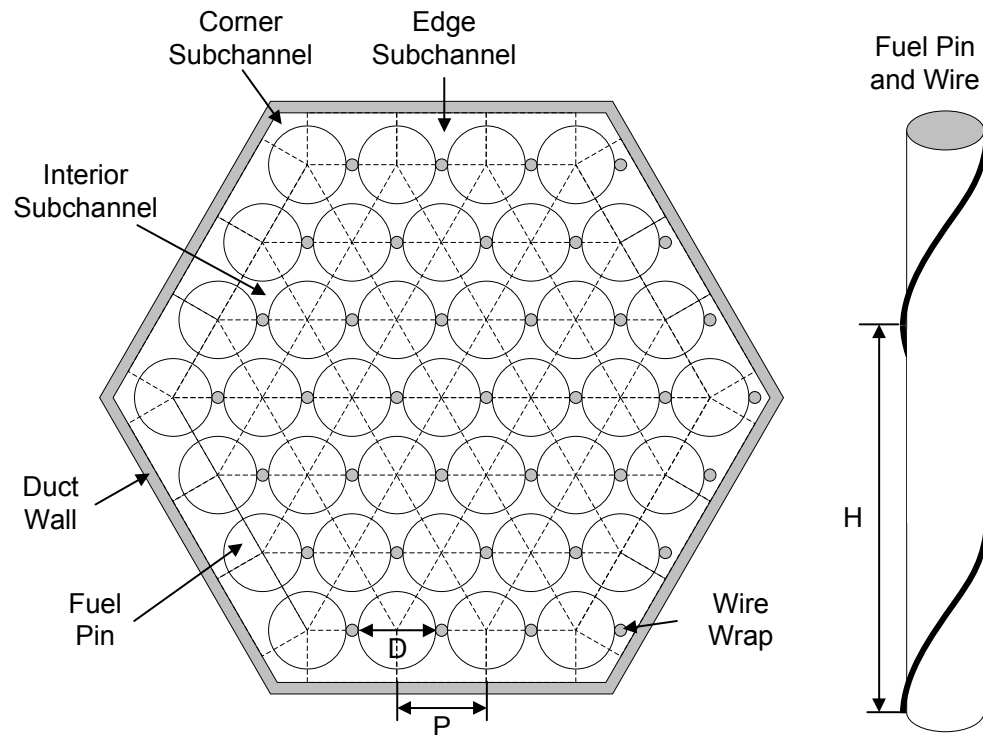


$N = 15$



Wire Wrapped Rod Bundles

- ❑ Uniformity of temperature controls peak power output
- ❑ A better understanding of flow distribution (interior, edge, corner) can lead to improved subchannel models.
- ❑ Wire wrap geometry is relatively complex



Single Rod in a Periodic Array, $Re=20,000$

$E=26000$, $N=7$, 8.7 M gridpoints

5 hours on P=2048 of 700 MHz BG/L for flow-through time.

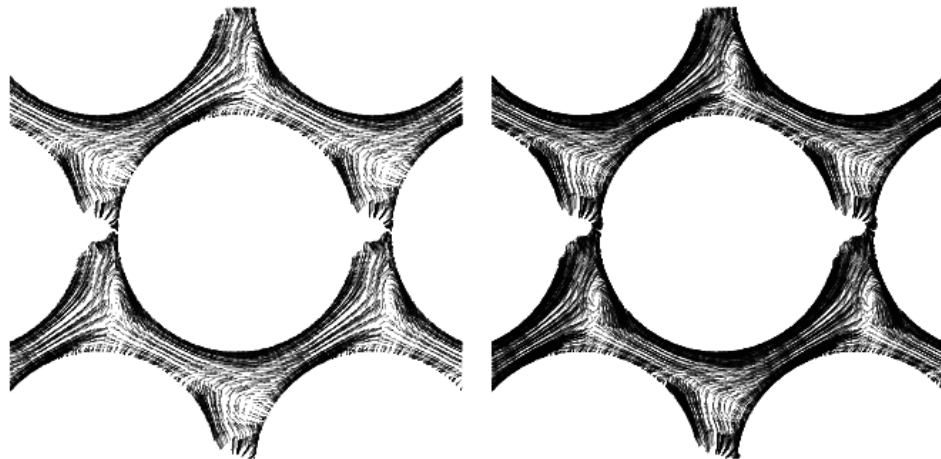
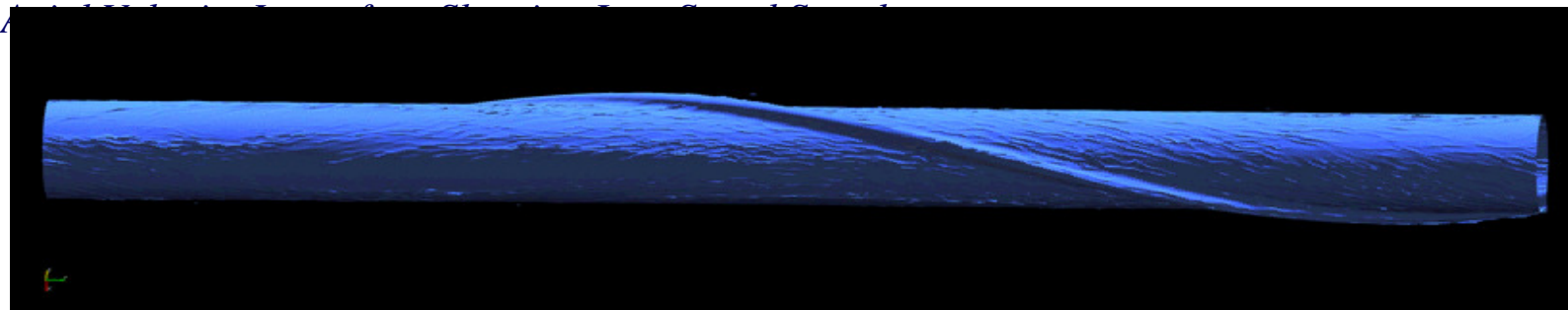
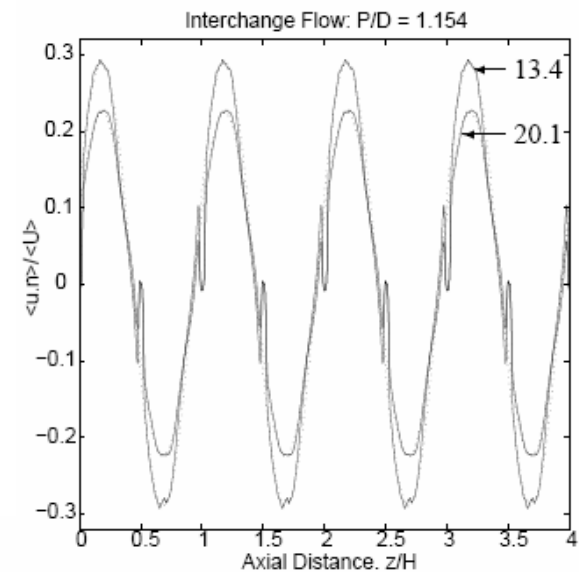


Figure 3. Mean velocity distributions at $z = 0$ for (left) $Re = 14052$, $H/D=20.1$, $N=7$ and (right) $Re = 28104$, $H/D=13.4$, $N=9$. Only 1/4 of the vectors are shown.



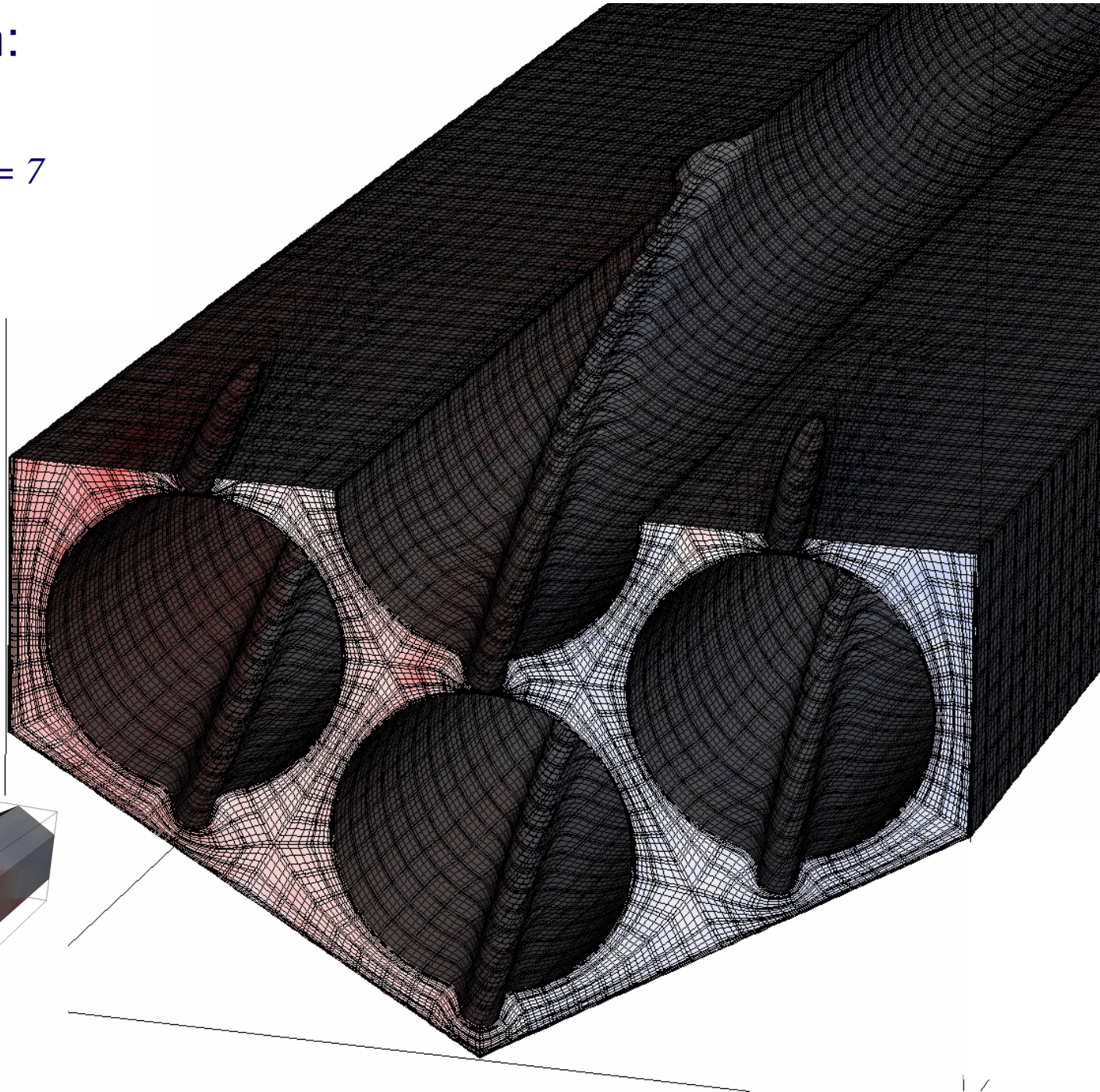
7 Pin Mesh:

$$E=132,000, N = 7$$

$$n_v \sim 44 M$$

$$n_p \sim 28 M$$

$$n_{iter} \sim 30 / step$$

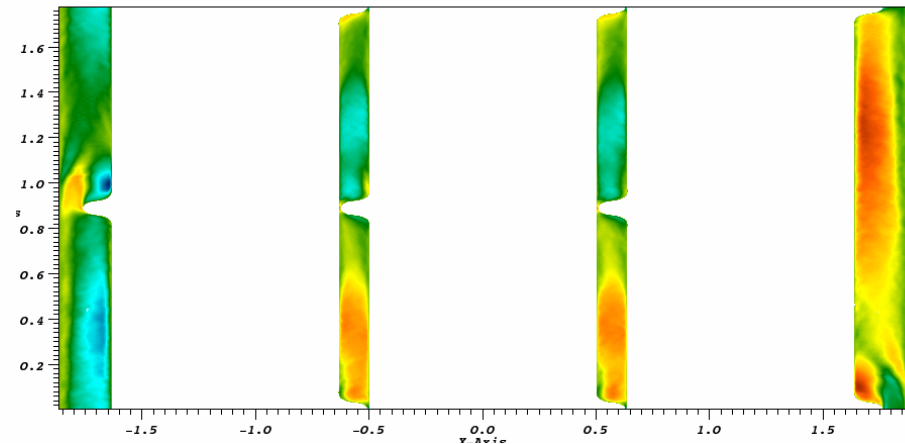
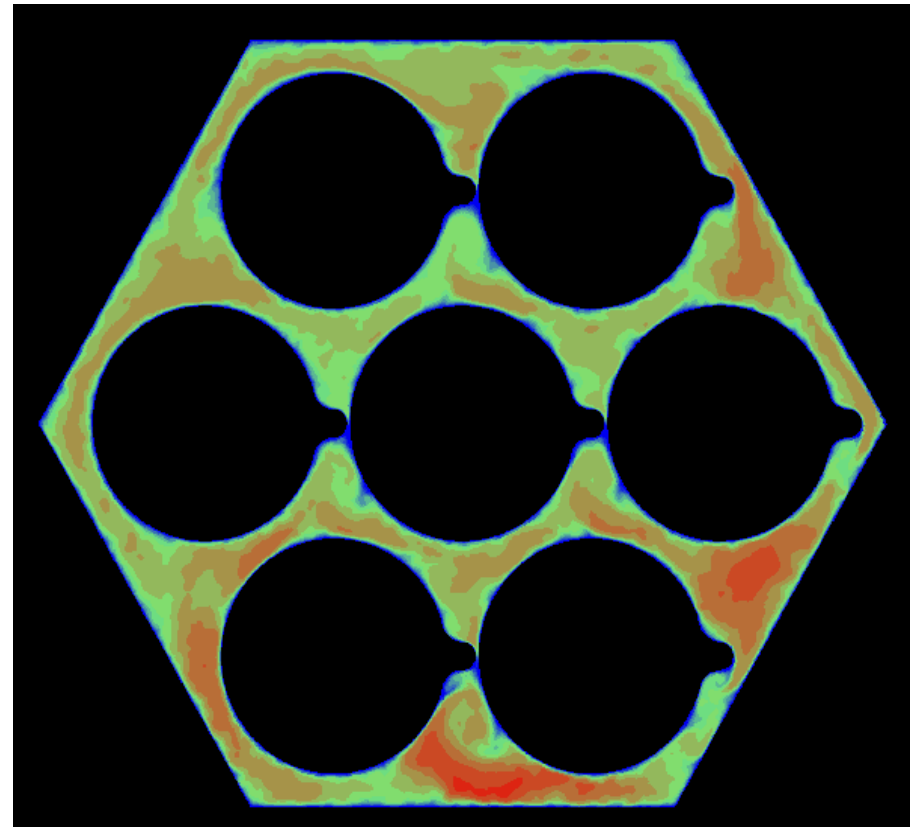
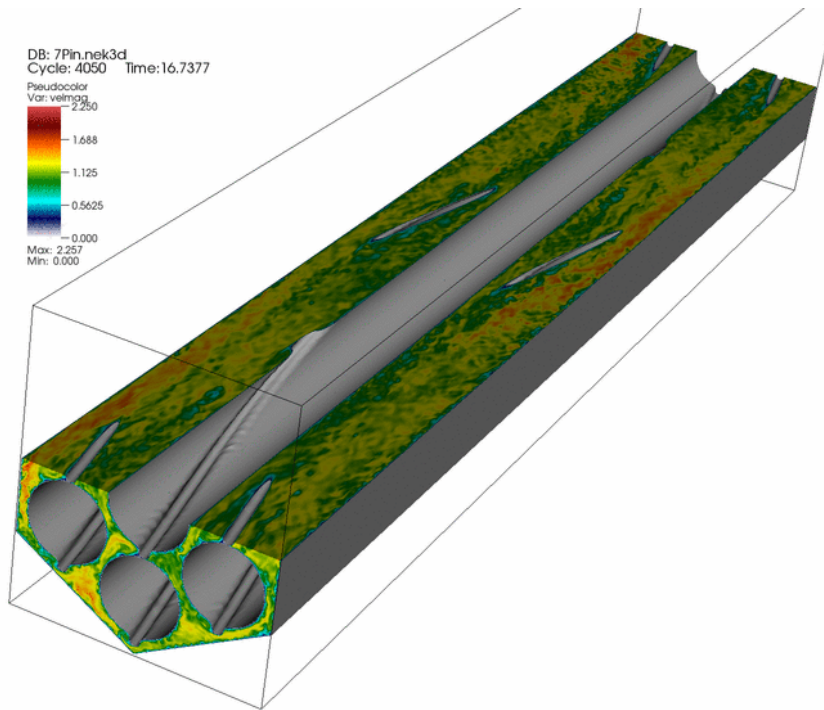


DB: 79W_nok3d
Cycle: 4050 Time: 16.7377
Pressure
Max: 0.750
Min: 0.000

7 Pin Configuration

Time-averaged axial (top) and transverse (bottom) velocity distributions.

Snapshot of axial velocity



Summary / Future Effort

- ❑ High-order SEM formulation
 - ❑ Stable formulation – dealiasing / filtering
 - Investigating relationship to SGS modeling (e.g., RT model, Schlatter '04, comparisons with D-Smagorinsky)
- ❑ Scalable solvers
 - ❑ Low iteration counts for typical “spectral-type” domains
 - ❑ Iteration counts higher for very complex geometries (e.g., multi-rod bundles) – work in progress
 - ❑ We will need to switch to AMG for coarse-grid solve *soon*
 $E > 100,000$; $P > 10,000$
- ❑ Future
 - ❑ Significant need for scalable, conservative, design codes
 - Developing conservative DG variant